Synthesis and Biological Activity of Fluorinated Combretastatin Analogues

Domenico Alloatti, Giuseppe Giannini,* Walter Cabri, Isabella Lustrati, Mauro Marzi, Andrea Ciacci, Grazia Gallo, M. Ornella Tinti, Marcella Marcellini, Teresa Riccioni, Mario B. Guglielmi, Paolo Carminati, and Claudio Pisano

R&D, Sigma-Tau Industrie Farmaceutiche Riunite S.p.A., Via Pontina Km 30.400, 00040 Pomezia, Italy

Received October 31, 2007

With the aim of understanding the influence of fluorine on the double bond of the *cis*-stilbene moiety of combretastatin derivatives and encouraged by a preliminary molecular modeling study showing a different biological environment on the interaction site with tubulin, we prepared, through various synthetic approaches, a small library of compounds in which one or both of the olefinic hydrogens were replaced with fluorine. X-ray analysis on the difluoro-CA-4 analogue demonstrated that the spatial arrangement of the molecule was not modified, compared to its nonfluorinated counterpart. SAR analysis confirmed the importance of the *cis*-stereochemistry of the stilbene scaffold. Nevertheless, some unpredicted results were observed on a few *trans*-fluorinated derivatives. The position of a fluorine atom on the double bond may affect the inhibition of tubulin polymerization and cytotoxic activity of these compounds.

Introduction

Combretastatin A-4 (CA-4[a]; compound **1** in Figure 1), a natural product first isolated in 1989 by G.R.Pettit et al.[1] from the bark of the South African bush willow, *Combretum caffrum*, is one of the most potent antimitotic agents. CA-4 shows strong cytotoxicity against a variety of cancer cells, including multidrug-resistant cell lines.[2] Several studies[3a,b] describe its ability to induce widespread necrosis of solid tumors.

It also exerts highly selective effects in proliferating endothelial cells and, as a consequence, demonstrates strong suppressive activity on tumor blood flow (TBF).[3c] Three derivatives are currently in clinical trials: CA-4 disodium phosphate (CA-4P; **4**), a water-soluble prodrug of CA-4 (**1**);[4,5] Oxi-4503, a water-soluble combretastatin A-1 prodrug (CA-1diP; **5**);[6,7] and AC7700 (**6**), also known as AVE8062 (Figure 1), an aminocombretastatin prodrug developed in Japan in 1998.[8,9]

As a result of the interesting activity of CA-4 and its analogues and the simplicity of its structure, a large number of derivatives were synthesized with the aim of extending structure−activity relationship (SAR) information to this class of molecules. As a consequence of these SAR analyses, the *cis*-stilbene scaffold of combretastatin appears distinct in three parts: (a) the trimethoxyphenyl moiety (A-ring), which influences cytotoxic activity; (b) the double bond that affects both cytotoxicity and tubulin binding; and (c) the B ring (phenol), which influences binding to tubulin.[2]

With respect to the double bond, the spatial relationship between the two aromatic rings of combretastatin, as well as that of colchicine and similar drugs, is an important structural feature that determines their ability to bind to tubulin. A large

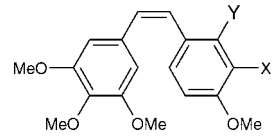

Drug	
1. X=OH, Y=H	CA-4
2. X=Y=OH	CA-1
3a. X=NO_2, Y=H	
3b. X=NH_2, Y=H	AVE-8063
Prodrug	
4. X=OPO_3Na_2, Y=H	CA-4P
5. X=Y=OPO_3Na_2	CA-1diP
6. X=NHCOCH(NH_2)CH_2OH, Y=H	AVE-8062-A

Figure 1. Natural and synthetic combretastatins with their corresponding water-soluble prodrug.

number of analogues with a modified bridge were synthesized. Saturation of the olefinic bridge (alkane derivatives),[2] as well as an increased unsaturation (alkyne derivatives),[10] reduce the cytotoxic and antitubulin activity of combretastatin. A loss of activity also occurs with the introduction of groups as large as −COOH, −CHO, CN, or larger groups, such as heterocyclic structures,[9,11,12,13a] with only a few exceptions.[13b]

The introduction of fluorine atoms into molecules of biological interest, such as steroids, carbohydrates, and others, proved beneficial. Antitumor agents, such as fluorouracil (EFUDEX), floxuridin (FUDR), tegafur (FENTAL), the more recently discovered gefitinib (IRESSA), camptothecin DX-8951f (Exatecan mesilate), and homocamptothecin (DN80915), are all examples of compounds harboring a fluorine atom. This growing interest is due to the unusual and unique chemical properties that fluorine can exert on the parent compound without altering its steric bulk.[14,15] Electron withdrawal by fluorine results in a strong polarization of the C−F bond, and the consequent pronounced electronic effects can have implications for reactions in adjacent centers and for drug−target interactions.[16] In addition, the incorporation of fluorine into a drug increases its lipophilicity, thus enhancing absorption into biological membranes, while the small covalent radius of fluorine can facilitate the docking of drugs with their receptor(s). The hydrophobic character of this covalent fluorine−carbon assembly is associated with a high dipole moment. This effect was recently described as polar hydrophobicity.[17] The increase in lipophilicity obtained by fluoroalkylation can be applied further to increase the binding properties of drug molecules to the hydrophobic regions of its target molecule. A lipophilic group attached to the ligand, which

* To whom correspondence should be addressed. Phone: +39-06-91393640. Fax: +39-06-91393638. E-mail: giuseppe.giannini@sigma-tau.it.

[a] Abbreviations: CA-4, combretastatin A-4; BMEC, bovine microvascular endothelial cells; MDR, multidrug resistance; DAMA-colchicine, *N*-deacetyl-*N*-(2-mercaptoacetyl)-colchicine; GDP, guanosine-5′-diphosphate; GTP, guanosine-5′-triphosphate; Ala, alanine; Asn, asparagine; Gln, glutamine; His, histidine; Val, valine; Thr, threonine; rms, root-mean-square; rmsd, root-mean-square deviation; H-bond, hydrogen bond; OPLS-AA, optimized potential for liquid simulations-all atom; TBDMSi, *tert*-butyl-dimethyl-silyl; DAST, diethylaminosulfur trifluoride; TBAF, tetra-*n*-butylammonium fluoride; ADME, absorption, distribution, metabolism and excretion; DMEM, Dulbecco's modified eagle medium; EDTA, ethylenediaminetetraacetic acid; PBS, phosphate-buffered saline; CCD, charge-coupled device.

10.1021/jm701362m CCC: $40.75
Published on Web 04/09/2008

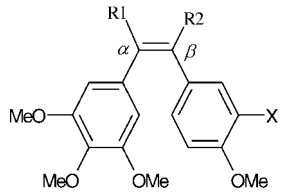

X= OH

7. R1, R2 = F (**ST2303**)
8. R1 = F, R2 = H (**ST2966**)
9. R1 = H, R2 = F (**ST3036**)
10. R1 = Br, R2 = F (**ST3000**)

X= NO_2

11. R1, R2 = F (**ST2998**)
12. R1 = F, R2 = H (**ST2969**)
13. R1 = H, R2 = F (**ST3038**)

X= NH_2

14. R1, R2 = F (**ST2996**)
15. R1 = F, R2 = H (**ST2971**)
16. R1 = H, R2 = F (**ST3040**)

X= F

17. R1 = H, R2 = F (**ST3001**)

Figure 2. Fluorinated combretastatins.

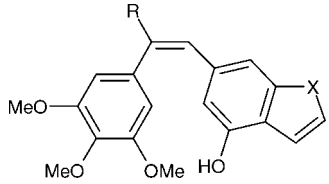

18. X=S R = F
19. X=O R = F

20. X=S R = H
21. X=O R = H

Figure 3. Fluorinated heterocombretastatins.

does not interfere with the active site of the enzyme to be inhibited, enhances its bioactivity upon binding to hydrophobic residues.

However, the introduction of fluorine atoms into a molecule is not always advantageous, as in the case of anthracyclines, where the introduction of fluorine atoms in different scaffold positions did not produce analogues in clinical development.[18] Prompted by the interesting results obtained with fluorinated colchicinoids against MDR cell lines,[19] the first fluorocombretastatins were synthesized by replacement of the hydroxyl[20,21] and/or methoxyl[22,23] on the B-ring, as well as by replacement of the methoxy group(s)[24] on the A-ring. There are also examples where fluorine was introduced into both rings.[21]

In addition, a fluorine on a stilbene-like double bond could influence the metabolic oxidation of this kind of molecular scaffold both on double bond and on phenolic ring (B-ring).[25] The introduction of a strong electron-withdrawing group, such as fluorine, could increase the metabolic survival of potentially bioactive molecules.

To explore the influence of fluorine substitution in the combretastatin series, we studied, in silico, and synthesized a small library of compounds in which one or both of the olefinic hydrogens were replaced with fluorine; to evaluate the influence of a different halogen, a monobromo monofluoro analogue was also synthesized (Figure 2).[26]

In addition, the same modifications were done on amino and nitro combretastatins, as well as on a new class of combretastatins recently synthesized in our laboratory,[27] in which the B-ring was replaced with benzofuran and benzothiophen heterocycles (Figure 3).

The fluorinated analogues, as well as reference compounds, were screened for their antiproliferative activity on bovine microvascular endothelial cells (BMEC); some of them were further tested for their antiproliferative activity on tumor cell lines and in the inhibition of tubulin polymerization.

Computational Chemistry. As a preparatory study of molecular modeling, we chose to evaluate, in silico, the influence of the fluorinated atom on the *cis*-stilbene double bond of the combretastatin scaffold. With this aim in mind, we started from known information about the colchicine binding site on a tubulin dimer.[28] The crystal structure shows five distinct protein subunits: two $\alpha\beta$-tubulin heterodimers and the stathmin-like domain of the regulatory protein, RB3. The colchicine binding site inhibitor, cocrystallized with each heterodimer, is *N*-deacetyl-*N*-(2-mercaptoacetyl)-colchicine (DAMA-colchicine).

To begin with, the stathmin-like domain and subunits A and B were removed. Subunits C and D were chosen because the 1-methoxy group of DAMA-colchicine of subunits A and B presented close contact with the side chain of Ala β316. The full $\alpha\beta$-tubulin complex, consisting of GDP, GTP-Mg^{2+}, and DAMA-colchicine, was used in the study. Bond order and formal charges were assigned to heteroatom groups. Hydrogen atoms were added to the entire system and the orientation of hydroxyl groups, amide groups of Asn and Gln, and the charge state of His residues were optimized. Subsequently, restrained minimization of the complex structure was performed until reaching an rms gradient of 0.1. The original X-ray structure and the refined complex had a heavy atom rms deviation (rmsd) of 0.28 Å, thus showing good stability despite an X-ray resolution of 3.58 Å. Indeed, the internal ligand docking showed a deviation from the X-ray coordinates of only 0.44 Å.

The molecular volume and electrostatic properties of the colchicine site impose severe constraints on the conformation of colchicine site inhibitors. Thus, we calculated a hydrophobic and hydrophilic map of the internal tubulin surface and molecular electrostatic potential surface for compounds **1**, **3a**, **3b**, **7**, **8a**, **9a**, and **11a–16a** to determine what would be the main contribution to binding affinity.

The cocrystallized inhibitor, DAMA-colchicine, was removed, and the accessible space in the active site was partitioned into three types of regions: hydrophobic (favorable to occupancy by hydrophobic ligand groups), hydrophilic (favorable to occupancy by hydrophilic ligand groups), and neither hydrophobic nor hydrophilic (of mixed character where at first approximation any type of group could reside with little effect on binding affinity). Hydrophobic and hydrophilic areas are 365.1 and 1413.4 $Å^2$, respectively. The middle portion of the active site is mainly hydrophobic (in magenta), while Figure 4a shows the peripheral section with a preferable hydrophilic (in light blue) characteristic.

Next, docking studies on the same compounds were carried out to investigate their binding mode. The trimethoxyphenyl group of OH and NH_2 derivatives move slightly from X-ray coordinates of the colchicine site (rmsd 1.7 Å), while the NO_2 derivative is located in close proximity (rmsd 1.2 Å). These shifts are necessary to accommodate the B-ring in the correct position to interact with Thr α179 or Val α181. As expected, fluorine introduction on the vinyl moiety is well-tolerated, promoting only little adjustment on the molecules. Figure 4b shows the docking-derived superposition of compounds **1**, **3a**, and **3b** (cyan, green, and orange, respectively). Comparing the hydrophobic and hydrophilic maps of the active site to the ligand docking solution, we can see that both phenyl groups of inhibitors are buried in the hydrophobic area. In addition, the Cα of the vinyl bridge is also completely embedded in the hydrophobic portion in contrast with the Cβ. Hence, the fluorine

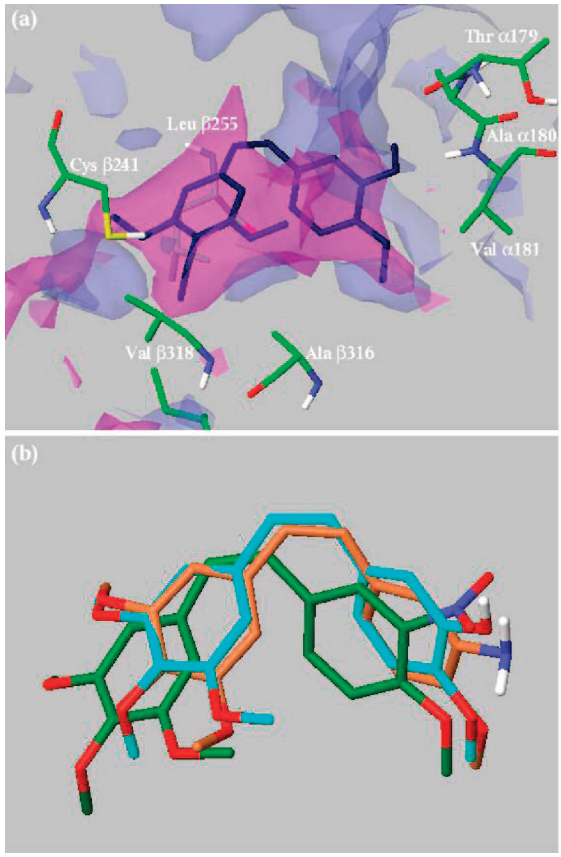

Figure 4. (a) CA-4 docked atop the colchicine-binding site. Hydrophobic (magenta) and hydrophilic (light blue) regions are shown. (b) Docking-derived superposition of **1** (cyan), **3a** (green), and **3b** (orange).

Table 1. Electrostatic Potential Values of Reference and Fluorinated Compounds

	electrostatic potential (kcal/mol)		
cmpd	min	max	2-MeO
1	−250.8	143.4	−247
7	−232.4	153	−225
8a	−243.3	147.4	−206
9a	−245.9	146.4	−243
3a	−302.4	298.3	−230
11a	−291.2	308.1	−216
12a	−293.3	294.3	−224
13a	−293.4	293.2	−229
3b	−256.9	122.5	−256.9
14a	−227.5	139.7	−227.5
15a	−235.3	129	−235.3
16a	−216.7	128.7	−216.7

position on the vinyl moiety could influence binding affinity in various ways.

To evaluate the electronic contribution of fluorine atom ligand substitution, we compared the electrostatic potential surfaces of different fluoro derivatives with the same substituent on the B-ring (see Supporting Information). In particular, we investigated the H-bond capability of OH and NH_2 as donor groups and the 2-methoxy group as acceptor. Electrostatic potential maps were calculated on the minimized docking-derived conformations. Table 1 reports some representative electrostatic potential values, where the H-bond donor capability (positive values) improves with respect to the number of fluorine atoms. On the contrary, the H-bond acceptor property (negative values) is negatively influenced by fluorine substitution, depending on its position and the B-ring substituent.

As a result of this study, we suggest that it might be interesting to explore how the different contributions (hydrophobic and electrostatic) of a fluorine atom on the vinyl double bond can influence tubulin binding.

Chemistry. Synthesis of Difluorocombretatastin. The difluorinated analogue of the naturally occurring CA-4 (**7**), together with its amino derivate (**14**), via the corresponding nitro (**11**), were synthesized using a route previously disclosed by Shimizu et al. for the preparation of difluorinated stilbenes.[29]

Addition of the carbenoid obtained in situ from tribromofluoromethane and BuLi in diethyl ether/THF 1:1 at –130 °C to the TBDMSi-protected isovanillin **22a** and to its nitro analogue **22b** gave the halogenated ethanols **23a** and **23b**, respectively. A DAST-mediated fluorination in dichloromethane afforded the difluoroethanes **24a** and **24b**.

Dehydrobromination-promoted lithium tetramethylpiperidine in diethyl ether/THF led us to the *cis* intermediates **25a** and **25b**, which were coupled under Suzuki conditions with commercially available 3,4,5-trimethoxybenzenboronic acid in refluxing toluene to give, after silyl deprotection or zinc reduction, final stilbenes **7** and **14** in good overall yields (Scheme 1).

Synthesis of Monofluorocombretastatin. As a first approach to the monofluorinated analogues, we chose a semisynthetic route which, after either a direct or bromohydrine-mediated (**29;** Scheme 2) bromofluorination, followed by a base-promoted elimination, would have led us to the desired monofluoro stilbenes.

As Scheme 2 describes, we used (*Z*)-4-methoxy-stilbene as our model compound and were able to obtain the desired fluorinated stilbenes in acceptable overall yields. Encouraged by this result, we applied the same protocol to CA-4 but obtained only low yields of the desired product, the major reaction observed being the bromination of the extremely activated A-ring. As a result, we adopted more reliable approaches for the two different regioisomers.

Synthesis of α-Fluorocombretastatin. The monofluorinated regioisomers of CA-4, **8**, and its amino derivative **15**, in which the fluorine atom is on the Cα (benzylic position with respect to the trimethoxyphenyl moiety), were prepared by using a fluorinated ylide strategy already explored by Burton et al.[30] The key step in this approach was the synthesis of the halogenated styrenes **31a** and **31b** from the reaction of isovanillin and aldehyde **22b** with the proper fluorinated ylide, generated in situ from triphenylphosphine and tribromofluoromethane in dichloromethane.

We obtained the desired styrenes in moderate yield as a 4:1 mixture of the geometric *E*- and *Z*-isomers, which were coupled with 3,4,5-trimethoxybenzenboronic acid. While for nitro derivative **12** we had no problem purifying the isomers, a zinc reduction in acetic acid gave **15** in good yields and isolation of the *E*-isomer of **32** needed a further silyl-protection step (**33**) to allow good chromatographic separation (Scheme 3).

Synthesis of *β*-Fluorocombretastatin. The addition of the carbenoid, obtained in situ from tetrabromomethane and BuLi in diethyl ether/THF 1:1 at –130 °C, to TBDMSi-protected isovanillin **22a** gave tribrominated alcohol **34** (Scheme 4), which after DAST-mediated fluorination and DBU-promoted elimination was converted to halogenated styrene **36** in good yield. This intermediate was converted to stilbene **38** following two alternative routes consisting of the same synthetic steps, with radical debromination and a Suzuki-coupling, but in different order.

Scheme 1. Synthesis of the Difluorinated Analogue of CA-4 and its Corresponding Nitro and Amino[a]

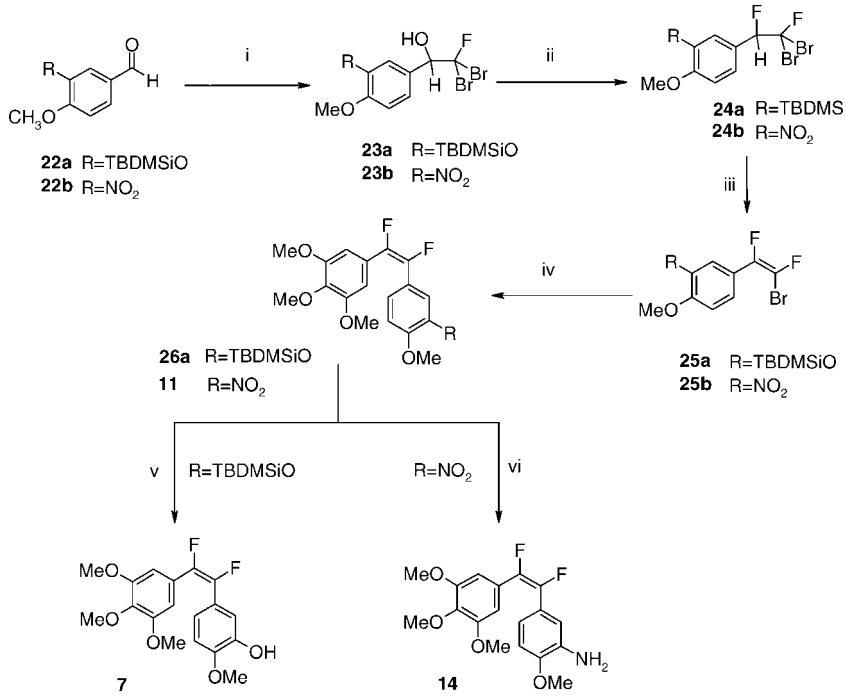

[a] Reagents and conditions: (i) $CFBr_3$, BuLi, Et_2O/THF, −130 °C, 2 h, 65%; (ii) DAST, CH_2Cl_2, −78°C, 2 h, 60%; (iii) tetramethylpiperidine, BuLi,THF/Et_2O, −100°C, 4 h, 59% (R = TBDMSiO), 30% (R = NO_2); (iv) 3,4,5-trimethoxybenzenboronic acid, 2 M Na_2CO_3, $Pd(PPh_3)_4$, refluxing toluene, 16 h, 83%; (v) TBAF, THF, 0 °C−RT, 2 h, 82%; (vi) Zn, AcOH, RT, 3 h, 80%.

Scheme 2. Study of Monofluoruration Using a (*Z*)-4-Methoxy-stilbene[a]

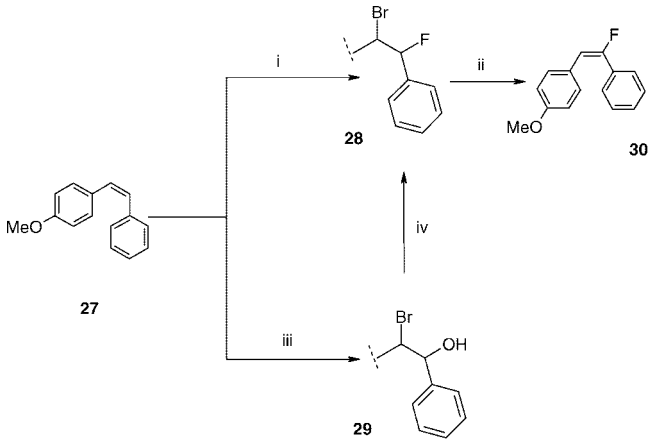

[a] Reagents and conditions: (i) NBS, HF•Pyr, CH_2Cl_2, Et_2O, −20 °C−RT, 1 h, 60%; (ii) DBU, DMSO, 80 °C, 3 h, 85%; (iii) NBS, CH_2Cl_2, −15°C, 1 h then 5% $NaHCO_3$, 40% (incomplete conversion); (iv) DAST, CH_2Cl_2, −78 °C−RT, 2 h, 78%.

The two routes proved to be almost comparable in efficiency, but the Pd-coupling on compound **36** showed a higher selectivity for *cis*-stilbene **37**, whose geometry was assessed by NOE experiments, compared to its *trans*-isomer (*cis*/*trans* ratio is 3:1). As a consequence, this synthetic route is slightly preferred. By deprotection of the silyl group of intermediate **37**, it is possible to obtain the α-bromo-*β*-fluorocombretastatin **10**, which was studied to explore the influence of a larger halogen on the double bond.

Removal of the TBDMSi-group with TBAF in THF gave the desired product **9** in good yield (Scheme 4).

Synthesis of *β*-Fluoroaminocombretastatin. An approach analogous to that used for the α-fluorocombretastatin was used for the synthesis of *β*-regioisomer of aminofluorocombretastatin **16**, starting from the commercially available 3,4,5-trimethoxybenzaldehyde **40** (Scheme 5).

The synthetic approach used for compound **8** allowed us to obtain the heterocyclic derivatives **18** and **19** (Scheme 6).

The use of a differently substituted boronic acid allowed us to obtain, directly from intermediate **41**, compound **17** (Scheme 7), which could be confronted with the reported analogue bearing no fluorine on the double bond.[21]

E/*Z*-Configuration of the synthesized compounds was assessed measuring the F−F coupling constants (^{19}F-NMR) for difluorinated compounds and the H−F coupling constants (^{1}H NMR) for monofluoro derivatives.

For selected fluorinated derivatives only, disodium phosphate prodrugs were synthesized according to the reported procedure,[31] and we report compound **43** as an example (Scheme 8) in the Experimental Section. These prodrugs are currently evaluated in in vivo models.

A crystal of **7**, suitable for X-ray analysis (Figure 5), was grown from a mixture of dichloromethane and hexane (1/2, v/v). The X-ray crystal structure revealed that the planes of the two phenyl rings were inclined toward each other, according to the nonfluorinated analogue structure.[32] Replacement of two olefinic hydrogens with fluorine did not modify the natural conformation of the CA-4.

Biological Results. The reference compound, as well as all synthesized compounds, was preliminarily tested for activity on bovine microvascular endothelial cells (BMEC).

The results in Table 2 show that all *trans*-stereoisomers were at least three times less-active than their *cis*-forms on BMEC. The *cis*-isomers were then evaluated for their interference with tubulin polymerization and tested on NCI-H460 non-small cell lung carcinoma and on HT29 colon carcinoma cells.

CA-4 (**1**) inhibited tubulin aggregation with an IC_{50} of 4.9 μM and has potent antiproliferative effect on endothelial cells

Scheme 3. Synthesis of C_α-Fluoro Analogues[a]

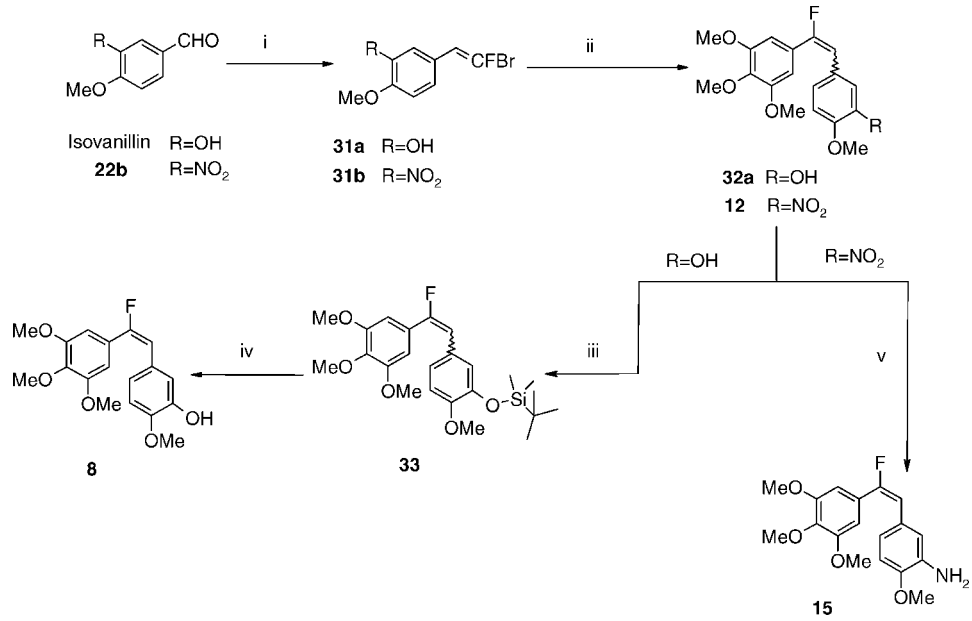

[a] Reagents and conditions: (i) $CFBr_3$, Ph_3P, CH_2Cl_2, RT, 2 h, 31%, *E*/*Z* = 4:1; (ii) 3,4,5-trimethoxybenzenboronic acid, $Pd(Ph_3P)_4$, 2 M Na_2CO_3, toluene, reflux, 44%, *E*/*Z* = 1:4; (iii) TBDMSiCl, imidazole, CH_2Cl_2, RT, 60%, chromatographic separation, *E*/*Z* = 1:4; (iv) 1 M TBAF, THF, 0 °C−RT, 2 h, 90%; (v) Zn, AcOH, RT, 16 h, 50%.

Scheme 4. Synthesis of C_β-Fluoro Analogues[a]

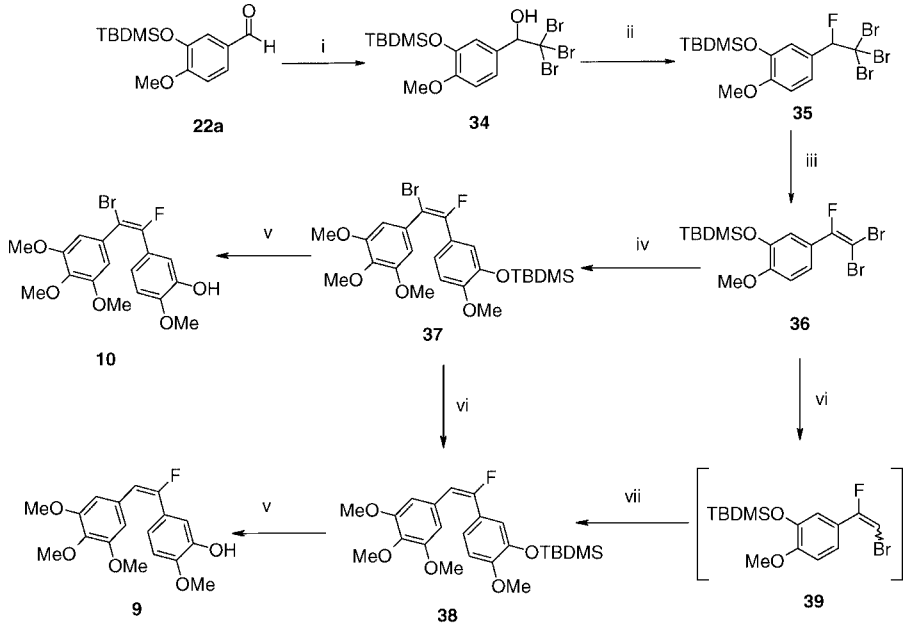

[a] Reagents and conditions: (i) $CFBr_4$, BuLi, THF, −78 °C, 2 h, 40%; (ii) DAST, CH_2Cl_2, −78 °C to RT, 2 h, 75%; (iii) DBU, RT, 4 h, 83%; (iv) 3,4,5-trimethoxybenzenboronic acid, 2 M Na_2CO_3, $Pd(PPh_3)_4$, refluxing toluene, 16 h, 31%; (v) TBAF, THF, 0 °C−RT, 2 h, 89%; (vi) AIBN, $BuSn_3H$, 80%; (vii) 3,4,5-trimethoxybenzenboronic acid, 2 M Na_2CO_3, $Pd(PPh_3)_4$, refluxing toluene, 16 h, 20%.

(IC_{50} = 2.6 nM), according to literature data.[27] Fluorine substitution into the double bond site in Cα position (**8a**) led to a 3-fold increment of tubulin disruption compared to that produced by one substitution in Cβ (**9a**) or in both positions (**7**), while this analogue (**8a**) produced a modest improvement in the inhibition of endothelial proliferation compared to CA-4 or its fluorine parent compounds. Moreover, it is interesting to note that the substitution of a fluorine with a bromine atom (**10**) resulted in a complete loss of activity compared to difluoro analogue **7**.

In comparison with NCI-H460 cells, HT29 colon carcinoma cells exhibited a certain degree of resistance to most of the fluorinated compounds with the 3-hydroxyl substitution on the B-ring, except for the **9a** derivative.

Replacement of the OH group with an NO_2 on the 3-position of the B-ring generated compounds such as **3a**, **11a**, and **13a**, which displayed similar potencies on tubulin polymerization compared to previous molecules, but a dramatic loss of antiproliferative activity in endothelial and tumor cells was observed. In this series, it was surprising that the presence of a

Scheme 5. Synthesis of C_β-Fluoroaminocombretastatin[a]

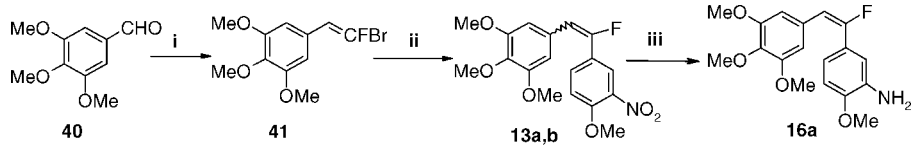

[a] Reagents and conditions: (i) $CFBr_3$, Ph_3P, CH_2Cl_2, RT, 2 h, 31%, *E*/*Z* = 1:1; (ii) 4-methoxy-3-nitrophenylboronic acid, $Pd(Ph_3P)_4$, 2 M Na_2CO_3, toluene, reflux, 56%, *E*/*Z* = 1:1.1; (iii) Zn, AcOH, RT, 2 h, 81% (starting from **13a**).

Scheme 6. Synthesis of C_α-Fluoro Heterocombretastatin[a]

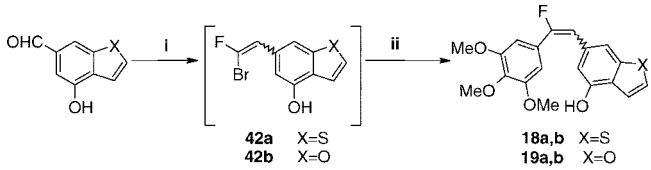

[a] Reagents and conditions: (i) $CFBr_3$, Ph_3P, CH_2Cl_2, RT, 2 h, 31%, *E*/*Z* = 4:1; (ii) 3,4,5-trimethoxybenzenboronic acid, $Pd(Ph_3P)_4$, 2 M Na_2CO_3, toluene, reflux, 44%, *E*/*Z* = 1:4.

fluorine atom in the Cα position of derivative **12a** produced an enhanced effect on tubulin aggregation, which correlated with a 4-fold increment in potency against endothelial and tumor cells compared to its reference **3a**.

Next, we examined the reference compound **3b**, which presented an NH_2 group on the 3-position of the B-ring and its fluorinated derivatives, **14a**, **15a**, and **16a**. Once again, fluorination on the Cα into the olefin site (**15a**) incremented the inhibition of tubulin polymerization three times, in comparison with the compounds produced by the other fluorinated amino analogues (**14a** and **16a**) but this constraint produced weak improvement of antiproliferative effect on endothelial and cancer cell lines, as compared to reference compound **3b**. On the contrary, although fluorination on the amino derivatives **14a** and **16a** resulted in a 3- to 5-fold loss in tubulin inhibition, the antiproliferative potency against endothelial and tumor cells was similar to that of **3b**. These last results confirm and extend previous observations reported in literature, in which a nonlinear relationship between proliferation inhibition and the effect on tubulin polymerization by compounds with the amino group in position 3′ were observed.[9]

Among the derivatives selected for further investigation, we chose the fluorinated nitro-analogue **12a**, which showed unexpected tubulin inhibitory activity and antiproliferative properties.

To evaluate the biological properties of this compound on BMEC cells, it was studied for its activity on the microtubule network and for its effect on cell cycle of BMEC, in comparison with CA-4. Cells were treated for 24 h at a concentration corresponding to IC_{80} to maximize the biological effects of compounds in asynchronously growing BMEC cells. Tubulin immunostaining showed that the **12a** molecule strongly affected the cell shape and microtubule arrangement in a manner comparable to CA-4 (Figure 6).

According to the effect on the microtubule cytoskeleton, flow cytometric data showed that **12a** had the same pattern as the reference compound, leading to an effective arrest of the cell cycle in the G_2/M phase and induction, to a significant extent, of apoptosis (Table 3).

Conclusions

The aims of this work were to devise a synthetic strategy to obtain mono and difluoro- derivatives of CA-4 and to verify the influence of these substitutions on antitumor activity. In addition, this strategy was justified by the preparatory data of the molecular modeling studies which suggested: a different environment for the two protons on double bond, more hydrophobic for H on Cα and more hydrophilic for H on Cβ, as well as the contribution of the fluorine in Cα position of the double bond, to H-bond acceptor and donor properties of the molecules.

Usually, to introduce fluorine atoms on the stilbene double bond in a regioselective manner, a semisynthetic approach is possible. However, this synthetic route is not feasible on combretastatin-like scaffolds, probably because of unfavorable electronic effects. Our studies provided a versatile synthetic approach, enabling us to obtain all the possible mono and difluoroderivatives of both the natural and the nitro/amino series. In addition, monofluorinated analogues of a new class of heterocombretastatins were obtainable via the same approach.

Scheme 7. Synthesis of C_β-Fluoro 3′-Deoxy-3′-fluoro CA-4[a]

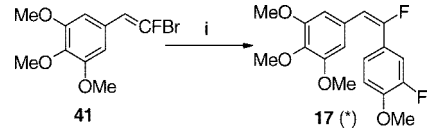

[a] Reagents and conditions: (i) 4-methoxy-3-fluorophenylboronic acid, $Pd(Ph_3P)_4$, 2 M Na_2CO_3, toluene, reflux, 62%, *E*/*Z* = 1.8:1. (*) The same synthetic sequence led to the *Z*-isomer.

Scheme 8. Synthesis of Disodium Phosphate Prodrug of the Difluorinated Analogue of CA-4[a]

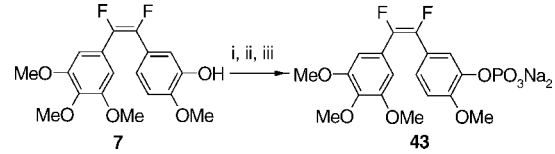

[a] Reagents and conditions: (i) $(BnO)_2P(O)H$, DIEA, CCl_4, CH_3CN, −25 °C, 88%; (ii) TMSCl, NaBr, CH_3CN, 2 h, RT; (iii) NaOH, H_2O, 15 h, 92% (two steps).

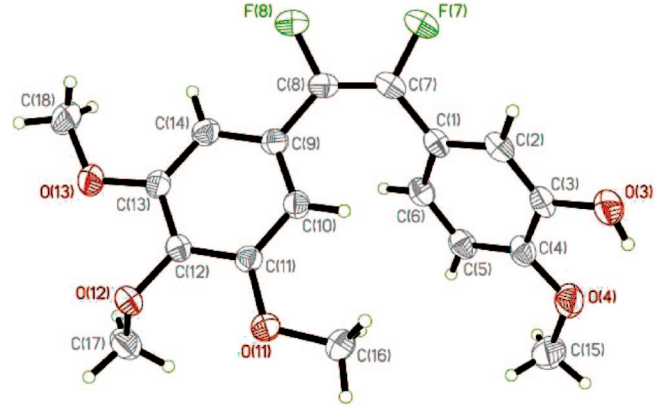

Figure 5. X-ray crystal structure of **7**.

Table 2. IC_{50} on Tubulin Polymerization and Cytotoxic Effect on BMEC, H460, and HT29 Cell Lines[g]

	code number	double bond geometry[a]	X	R1, R2	inhibition of tubulin aggregation[b]	BMEC[c]	H-460[d]	HT29[e]
1	CA-4	*A*	OH	H, H	4.9 ± 0.2	2.6 ± 0.21	1.24 ± 0.02	118 ± 0.03
7	ST2303	*A*	OH	F, F	7.3 ± 0.3	4.6 ± 0.5	3.0 ± 0.05	110 ± 0.01
8a	ST2966	*A*	OH	F, H	2.5 ± 0.1	1.7 ± 0.6	1.1 ± 0.02	100 ± 11
8b	ST2967	*B*	OH	F, H		13 ± 2.7		
9a	ST3036	*A*	OH	H, F	8.8 ± 0.1	4.7 ± 0.1	4 ± 0.2	28.9 ± 3.7
9b	ST3037	*B*	OH	H, F		26.6 ± 2.4		
10	ST3000	*A*	OH	Br, F		>200		
3a	ST3098	*A*	NO_2	H, H	6.8 ± 0.1	135 ± 1.3	128 ± 0.6	113 ± 1
11a	ST2998	*A*	NO_2	F, F	8.2 ± 0.2	749 ± 75	1166 ± 75	1307 ± 26
11b	ST2999	*B*	NO_2	F, F		2300 ± 53		
12a	ST2969	*A*	NO_2	F, H	2.3 ± 0.3	38.4 ± 2.5	42.6 ± 6	32 ± 6.5
12b	ST2970	*B*	NO_2	F, H		2800 ± 72		
13a	ST3038	*A*	NO_2	H, F	10.9 ± 1.5	329 ± 2.5	379 ± 0.2	202 ± 19
13b	ST3039	*B*	NO_2	H, F		>3000		
3b	ST3100	*A*	NH_2	H, H	3.5 ± 0.2	3.1 ± 0.4	4.9 ± 0.1	5 ± 0.5
14a	ST2996	*A*	NH_2	F, F	17.5 ± 1.4	3.6 ± 0.2	7.3 ± 0.9	4.5 ± 0.1
14b	ST2997	*B*	NH_2	F, F		204 ± 5.4		
15a	ST2971	*A*	NH_2	F, H	5.5 ± 0.1	2.0 ± 0.8	2.4 ± 0.2	2.9 ± 0.02
15b	ST2972	*B*	NH_2	F, H		86 ± 1.3		
16a	ST3040	*A*	NH_2	H, F	13.7 ± 0.6	2.1 ± 0.2	11.5 ± 0.9	5 ± 0.3
16b	ST3041	*B*	NH_2	H, F		111 ± 15		
17a	ST3001	*A*	F	H, F		23 ± 1.3[f]		
17b	ST3002	*B*	F	H, F		610 ± 15		

[a] For general structure, see Figure 2. [b] A: *Z*-stilbene scaffold; B: *E*-stilbene scaffold. [c] IC_{50} [IC_{50} ± SD; μM]. [d] Bovine microvascular endothelium [IC_{50} ± SD; nM]. [e] Lung carcinoma [IC_{50} ± SD; nM]. [f] Colon carcinoma [IC_{50} ± SD; nM]. Data represent the means of at least three experiments. [g] For the dehalogenated compound, ref 21 reports IC_{50} = 10 nM and IC_{50} = 4 nM on K562 and HUVEC cell lines, respectively.

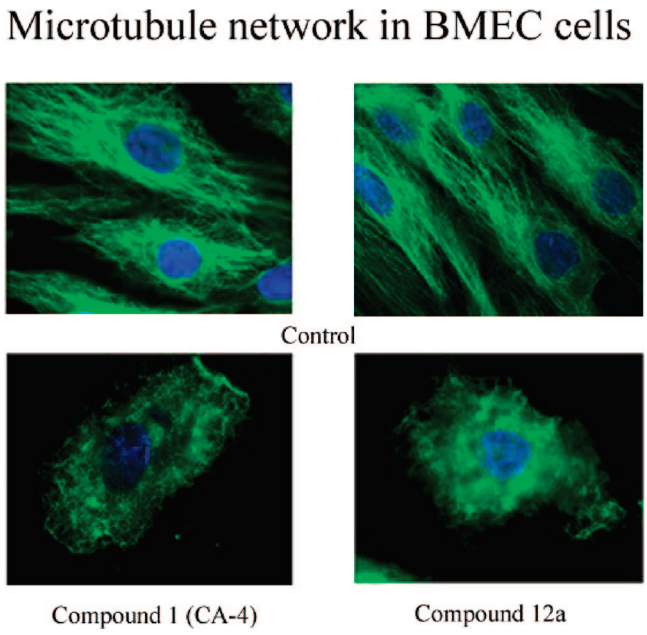

Figure 6. Immunostaining experiments on **1** and **12a**. α-Tubulin (green) and nuclear staining (blue) of cells after 24 h of drug treatment. Magnification: 100×.

Table 3. Flow Cytometric Analysis of Apoptosis and Cell Cycle of NCI-H460 Cells[a]

	$G_{0/1}$%	S%	G_2/M%	apoptosis ($subG_1$)%
untreated	44.2	39.9	16.0	0.8
cmpd **1** (CA-4)	4.9	8.6	86.4	20.5
cmpd **12a**	3.2	9.8	87.1	18.4

[a] NCI-H460 cells were exposed for 24 h to the compounds (IC_{80} dose), stained with propidium iodide, and processed on a FACScan flow cytometer. Cell cycle distribution and apoptosis were assessed as described in Experimental Section.

Taken together, this study demonstrates that it is possible to introduce one or two fluorine atoms on the stilbene double bond of combretastatins without altering their biological properties. In fact, the monofluoro- and difluoro- derivatives showed in vitro properties overlapping those of the parent compounds. Nevertheless, small differences can be observed, which always remain in the low nanomolar range. The introduction of a fluorine atom, both in Cα and in C*β*, (**7**), or only in C*β* (**9a**), results in a slight reduction of tubulin aggregation. On the contrary, when the fluorine atom was introduced only on Cα (**8a**) an improvement of activity was observed when compared to the parent compound (**1**). And the same trend, more potent with fluorine on Cα and less potent with fluorine on C*β* or Cα−C*β*, was observed for nitro (**11a**, **12a**, **13a**) and amino (**14a**, **15a**, **16a**) derivatives.

The same effect was observed as cytotoxic activity, both on the endothelial (BMEC) and tumor cell lines (H-460).

On the HT29 tumor cell line, which is naturally less responsive to combretastatin (**1**) and to nitrocombretastatin (**3a**) but sensitive to aminocombretastatin (**3b**), introduction of fluorine showed an equivalent trend (more potent with fluorine on Cα) limited to nitro-(**11a**, **12a**, **13a**) and amino-(**14a**, **15a**, **16a**) derivatives. An exception to this trend was observed for the natural scaffold where the most efficacious substitution was in C*β* (**9a**).

The biological results seem to be in agreement with the previous observation, in terms of different biological environments regarding the interaction of Cα and C*β* (see Figure 4a).

The substitution of fluorine with bromine on Cα (compound **10**) resulted in a 40-fold reduction in antiproliferative activity on the BMEC cell line with respect to the parent compounds **7** and **9a**. This data confirm the negative influence of steric factors on the double bond of the stilbene scaffold.

A reduction in antiproliferative activity against BMEC was observed when the phenolic OH of **9a/b** was substituted with a second fluorine atom to give compound **17a/b**.

The *trans*-stilbene scaffold is known to be much less potent, compared to the corresponding *cis*. The same trend was observed for our fluorinated derivatives, with some exceptions. Indeed, derivatives **8b**, **9b**, and to a lesser extent **14b**,**15b**, and **16b**, still possessed a nanomolar activity although endowed with a minor antiproliferative potency with respect to **1**. To explain these biological data, one hypothesis considers the influence of

fluorine on *trans*-double bond stability and on the possible facilitation of reduction of the nitro group with respect to the corresponding amino derivative. Thus, these unpredictable results encourage further investigation.

One of the synthetic procedures exploited in this paper was used to synthesize the fluorinated (on Cα) analogues (**18** and **19**) of a novel class of heterocombretastatins previously developed in our laboratories.[27] Preliminary unpublished results seem to confirm, even for these compounds, that the introduction of fluorine does not significantly affect biological activity (see Supporting Information).

The biological data collected up to now show that the introduction of one/two fluorines on the double bond of combretastatin, unlike the introduction of bulkier groups, does not appreciably influence the biological response of most of the synthesized compounds. Therefore, according to what is already described for other fluorinated drugs,[33] it may be reasonable to observe differences in pharmacokinetic and metabolic properties with respect to the nonfluorinated analogues. An ADME (absorption, distribution, metabolism, and excretion) analysis is currently under investigation and will be reported in due course.

Experimental Section

Computational Chemistry. Compounds **1**, **3a**, **3b**, **7**, **8a**, **9a**, and **11a**−**16a**, structural analogues of CA-4, were selected for this study. The X-ray structure of the αβ tubulin-DAMA-colchicine complex (pdb code 1SA0, chains C and D)[28] was used; said complex was subjected to the standard protein preparation procedure implemented in Maestro.[34] The hydrophobic and hydrophilic surfaces of the colchicine binding site were calculated with Maestro hydrophobic/philic facility. The active-site mapping procedure operates in a manner analogous to Goodford's GRID algorithm.[35] "Hydrophilic" and "hydrophobic" regions are defined in a way that considers both spatial proximity to the receptor and suitability for occupancy by solvent–water. The first step in the computing grid is to define a rectilinear box that contains an active site and to define grid points with a typical grid spacing of 1 Å within the box. Next, van der Waals energies and *x*, *y*, and *z* electrostatic field components are computed at each of the grid points. Receptor atom partial charges and van der Waals parameters are taken from the OPLS-AA force field.[36] A probe is represented by a van der Waals sphere of radius 1.5 Å and well depth of 0.2 kcal/mol and has a point dipole moment of 2.3 debye.[37,38] The 3D structure of the ligands was energy minimized using Macromodel (500-step truncated Newton conjugated gradient with convergence threshold 0.01).[39] Semiempirical PM3 charges and electrostatic potential maps were calculated with the Spartan '06 software.[40] As reported in literature,[41] we correlated the hydrogen bond capability of OH, NH_2, and the 2-methoxy groups to the maximum and minimum values, respectively, of electrostatic potential.

Docking was carried out with Glide software.[42] Docking procedure was first constituted by receptor grid generation: two cubic boxes centered on the cocrystallized DAMA-colchicine were created with a range of 24 and 10 Å, respectively, on each side. Ligands were docked flexibly using default scaling for van der Waals radii and setting multiple solutions for each molecule.[43] Postdocking minimization was performed using MM-GBSA approach,[44] implemented in Prime software,[42] with the rigid receptor approximation. OPLS-AA force field was used in both calculations.

Chemistry. General Remarks: ^{1}H-, ^{13}C-, and ^{19}F-NMR spectra were recorded, unless otherwise indicated, in $CDCl_3$ solution at 200- or 300-MHz on a Varian Gemini-200 or a Varian Gemini-300 instrument. Chemical shift values are given in ppm and coupling constants in Hz. Melting points were determined on a Mettler DSC-30 and are uncorrected. Electro-Spray mass spectra were recorded on a Waters Micromass ZQ-2000 instrument. Thin layer chromatography (TLC) was carried out using Merck precoated silica gel F-254 plates. Flash chromatography was done using Merck silica gel 60 (0.063–0.200 mm). Solvents were dried according to standard procedures and reactions requiring anhydrous conditions were performed under argon. Solutions containing the final products were dried with Na_2SO_4, filtered, and concentrated under reduced pressure using a rotatory evaporator. All the final products undergoing biological testing were analyzed in a Jasco HPLC system consisting of two PU-2080 pumps and an MD-2010 detector, with purity above 99%. Microanalysis of all new synthesized compounds was within ±0.4% of calculated values.

***tert*-Butyl-dimethyl-silyl Isovanillin (22a).** To a solution of 6.09 g (40 mmol) of isovanillin in 50 mL of CH_2Cl_2 were added 6.64 g of TBDMSiCl (44 mmol, 1.1 equiv) and 2.95 g (44 mmol, 1.1 equiv) of imidazole. The solution was stirred at room temperature for three h and then washed with 0.5 M HCl. The crude product was purified on a silica gel column using hexane/ethyl acetate 9:1, to give 9 g (33 mmol, 83%) of a colorless oil. R_f = 0.27 (hex./ethyl acetate 95:5). MS (IS): $[MH]^+ = 267.2$ $[M + Na]^+ = 289.2$ (main peak). ^{1}H NMR (200 MHz, $CDCl_3$, δ): 0.20 (s, 6H, 2xCH_3); 1.03 (s, 9H, tBu); 3.92 (s, 3H, OCH_3); 6.98 (d, J = 8.4 Hz, 1H, CH); 7.39 (d, J = 2.2 Hz, 1H, CH); 7.50 (dd, J = 8.4 Hz, J = 2.2 Hz, 1H, CH); 9.84 (s, 1H, CHO). Anal. ($C_{14}H_{22}O_3Si$) C, H.

2,2-Dibromo-2-fluoro-1-(4-methoxy-3-*tert*-butyl-dimethyl-silyloxyphenyl) Ethanol (23a). A mixture of 2.66 g (10 mmol) of TBDMS-isovanillin **22a** and 2.98 g (11 mmol, 1.1 equiv) of $CFBr_3$ in 80 mL of Et_2O/THF (1:1) was brought to T = −130 °C; 4.4 mL (11mmol, 1.1 equiv) of a 2.5 M BuLi solution in hexane was added to the mixture in ten min. After two h at T = −70 °C, it was necessary to add 1.3 mL of BuLi solution and 0.3 mL of $CFBr_3$ to drive the reaction to completion. The reaction was quenched with 60 mL of NH_4Cl saturated solution and diluted with 20 mL of diethyl ether. The aqueous phase was back-extracted with 2 × 20 mL of diethyl ether, and the organic fractions were collected, dried over anhydrous sodium sulfate, and then purified on a silica gel column using hexane/ethyl acetate 95:5 to give 3.1 g (6.8 mmol, 68%) of a waxy solid. R_f = 0.5 (hex/AcOEt 85:15). MS (IS): $[M + Na]^+ = 479.1$; 481.1; 483.1 (1:2:1). ^{1}H NMR (200 MHz, $CDCl_3$, δ): 0.18 (s, 6H, 2 × CH_3); 1.01 (s, 9H, tBu); 3.84 (s, 3H, OCH_3); 5.03 (d, J = 9.5 Hz, 1H, CH,); 6.87 (d, J = 8.4 Hz, 1H, CHar); 7.09 (m, 2H, 2 × CH). Anal. ($C_{15}H_{23}Br_2FO_3Si$) C, H.

1,1-Dibromo-1,2-difluoro-2-(4-methoxy-3-*tert*-butyl-dimethyl-silyloxyphenyl)ethane (24a). (Diethylamino)sulfur trifluoride at 1.5 mL (11.2 mmol; 1.8 equiv) in 10 mL CH_2Cl_2 was added to a solution of 2.84 g (6.2 mmol) of alcohol **23a** in 14 mL of CH_2Cl_2 at −78 °C. The reaction mixture was allowed to warm up to 0 °C over a period of two h, quenched with 25 mL of $NaHCO_3$ saturated solution and diluted with 20 mL of diethyl ether. The organic phase was dried over anhydrous sodium sulfate and purified on preparative TLC using hexane/ethyl Acetate 98:2 to give 1.8 g (4 mmol; 64.5%) of a yellow oil. R_f = 0.43 (hex./AcOEt 97:3). MS (IS): $[M + Na]^+ = 483.1$; 485.1; 487.1 (1:2:1). ^{1}H NMR (200 MHz, $CDCl_3$, δ): 0.18 (s, 6H, 2 × CH_3); 1.02 (s, 9H, tBu); 3.86 (s, 3H, OCH_3); 5.59 (dd, J = 43.6 Hz, J = 11.0 Hz, 1H, CH,); 6.89 (d, J = 8.4 Hz, 1H, CHar); 7.06 (s, 1H, CH); 7.10 (d, J = 8.4 Hz, 1H, CH). Anal. ($C_{15}H_{22}Br_2F_2O_2Si$) C, H.

(*E*)-1-Bromo-1,2-difluoro-2-(4-methoxy-3-*tert*-butyl-dimethyl-silyloxyphenyl)ethene (25a). *Step 1*. Preparation of the tetramethylpiperidide solution. Dissolved in 4 mL of anhydrous THF were 1.9 mL (11.7 mmol; 3 equiv) of 2,2,6,6-tetramethylpiperidine; the solution was cooled to −80 °C and then 3.9 mL (9.8 mmol; 2.5 equiv) of a 2.5 M solution BuLi in hexane were added. The mixture was stirred for 2 h at 0 °C. *Step 2*. Dehydrobromination. A solution of 1.8 g (3.9 mmol) of compound **24a** in 5 mL of anhydrous THF was added to the tetramethyl piperidide solution previously cooled down to −100 °C. After 1 h, the reaction was washed with 10 mL of HCl (0.1 N), and the aqueous phase was back-extracted with 2 × 10 mL Et_2O. The organic extracts were collected and dried over anhydrous sodium sulfate and then purified on preparative silica plates with *n*-hexane/ethyl acetate 97:3 to give 857 mg (2.3 mmol; 59%) of product as a pale yellow oil. According to the final product

7 configuration (assigned by ^{19}F-NMR), the stereochemistry of the two fluorines on the double bond was *cis*. $R_f = 0.8$ in hex/acetone 8:2. MS (IS): $[M + Na]^+ = 401.4$; 403.4 (1:1). ^{1}H NMR (200 MHz, $CDCl_3$, δ): 0.19 (s, 6H, 2 × CH_3); 1.02 (s, 9H, tBu); 3.86 (s, 3H, OCH_3); 6.88 (d, $J = 8.4$ Hz, 1H, CH); 7.16 (d, $J = 2.2$ Hz, 1H, CH); 7.23 (dd, $J = 8.4$ Hz, $J = 2.2$ Hz, 1H, CH). Anal. ($C_{15}H_{21}BrF_2O_2Si$) C, H.

(*Z*)-1,2-Difluoro-1-(3,4,5-trimethoxyphenyl)-2-(4-methoxy-3-*tert*-butyl-dimethyl-silyloxyphenyl)ethene (26). A mixture of 750 mg (1.98 mmol; 1 equiv) of stirene **25a**, 1.260 g (5.94 mmol; 3 equiv) of 3,4,5-trimethoxyphenylboronic acid, 4 mL of Na_2CO_3 2 M aqueous solution and 104 mg (0.09 mmol; 0.05 equiv) of $Pd(Ph_3P)_4$ in 20 mL of toluene was refluxed overnight. The solution was then cooled down to room temperature, dried over anhydrous sodium sulfate, and the crude mixture was passed through a short silica gel column to remove catalyst. The crude product was purified by chromatography on silica gel plates with hexane/acetone 8:2 to give 740 mg (1.6 mmol; 81%) of a colorless oil. $R_f = 0.36$ in hex/acetone 8:2. MS (IS): $[M + NH_4]^+ = 484.1$; $[2M + NH_4]^+ = 950.1$. ^{1}H NMR (200 MHz, $CDCl_3$, δ): 0.08 (s, 6H, 2 × CH_3); 0.94 (s, 9H, tBu); 3.71 (s, 6H, 2 × OCH_3); 3.82 (s, 3H, OCH_3); 3.86 (s, 3H, OCH_3); 6.57 (s, 2H, 2 × CH); 6.81 (d, $J = 8.4$ Hz, 1H, CH); 6.84 (q, $J = 2.2$ Hz, $J = 0.8$ Hz, 1H, CH); 7.00 (dq, $J = 8.4$ Hz, $J = 2.2$ Hz, $J = 0.8$ Hz, 1H, CH). Anal. ($C_{24}H_{32}F_2O_5Si$) C, H.

(*Z*)-1,2-Difluoro-1-(3,4,5) trimethoxyphenyl)-2-(3-hydroxy-4-methoxyphenyl)ethene (7). A 1 M solution of tetrabutylammonium fluoride in THF (9.4 mmol; 2 equiv) was dripped, at 0 °C and under inert atmosphere, into a solution of 2.2 g (4.7 mmol) of stilbene **26** in 10 mL of anhydrous THF (stored on molecular sieves). The reaction mixture was allowed to warm up to room temperature and the reaction completed after four h. The mixture was poured onto ice, the aqueous phase extracted with Et_2O (3 × 20 mL); the organic extracts were collected and dried over anhydrous Na_2SO_4. The crude mixture was purified by chromatography on silica gel with *n*-hexane/acetone 8:2 to give 1.361 g (3.9 mmol; 83%) of a white solid; mp = 134–137 °C. MS (IS): $[M + H]^+ = 353.0$. ^{1}H NMR (200 MHz, $CDCl_3$, δ): 3.71 (s, 6H, 2 × OCH_3); 3.87 (s, 3H, OCH_3); 3.91 (s, 3H, OCH_3); 5.64 (s, 1H, OH); 6.58 (s, 2H, 2 × CH); 6.80 (d, $J = 8.4$ Hz, 1H, CH); 6.91 (dq, $J = 8.4$ Hz, $J = 2.2$ Hz, 1.1 Hz, 1H, CH); 7.00 (d, $J = 2.2$ Hz, 1H, CH). ^{19}F NMR (282 MHz, $CDCl_3$, δ): −126.2 (d, JFF = 14.8 Hz), −130.3 (d, JFF = 14.8 Hz). Anal. ($C_{18}H_{18}F_2O_5$) C, H.

2,2-Dibromo-2-fluoro-1-(3-nitro-4-methoxy-phenyl)ethanol (23b). The same procedure used for compound **23a**, after purification on a silica gel column using hexane/ethyl acetate 95:5, gave 1.146 g (3.1 mmol, 57.4%) of a yellow oil. $R_f = 0.53$ (hex/AcOEt 6:4). MS (IS): $[M - 1]^- = 371.8$. ^{1}H NMR (200 MHz, $CDCl_3$, δ): 3.2 (bs, 1H, OH); 4.0 (s, 3H, OCH_3); 5.15 (dd, $J = 2.9$ Hz, $J = 8.0$ Hz, 1H, CH); 7.13 (d, $J = 8.8$ Hz, 1H, CHar); 7.76 (dd, $J = 8.8$ Hz, $J = 2.2$ Hz, 1H, CHar); 8.10 (d, $J = 2.2$ Hz, 1H, CHar). Anal. ($C_9H_8Br_2FNO_4$) C, H, N.

1,1-Dibromo-1,2-difluoro-2-(3-nitro-4-methoxy-phenyl) Ethane (24b). The same procedure used for compound **24a**, after purification on a silica gel column using hexane/ethyl acetate 7:3, gave 960 mg (2.6 mmol; 84%) of a yellow oil. $R_f = 0.493$ (hex/AcOEt 7:3). ^{1}H NMR (200 MHz, $CDCl_3$, δ): 4.03 (s, 3H, OCH_3); 5.71 (dd, $J = 43.2$ Hz, $J = 9.5$ Hz, 1H, CH,); 7.18 (d, $J = 8.8$ Hz, 1H, CHar); 7.76 (dd, $J = 8.8$ Hz, $J = 1.8$ Hz, 1H, CHar); 8.08 (d, $J = 1.8$ Hz, 1H, CHar). Anal. ($C_9H_7Br_2F_2NO_3$) C, H, N.

(*Z*)-1-Bromo-1,2-difluoro-2-(3-nitro-4-methoxy-phenyl)-ethene (25b). The same procedure used for compound **25a**, after purification on a silica gel column using hexane/ethyl acetate 8:2, gave 100 mg (0.34 mmol; 13%) of product as a yellow oil. $R_f = 0.36$ in hex/acetone 8:2. MS (IS): $[M + Na]^+ = 315.8/317.8$. ^{1}H NMR (200 MHz, $CDCl_3$, δ): 4.03 (s, 3H, OCH_3); 7.18 (d, $J = 9.2$ Hz, 1H, CHar); 7.78 (dd, $J = 9.2$ Hz, $J = 2.6$ Hz, 1H, CHar); 8.09 (d, $J = 2.6$ Hz, 1H, CHar). Anal. ($C_9H_6BrF_2NO_3$) C, H, N.

(*Z*/*E*)-1,2-Difluoro-1-(3,4,5-trimethoxyphenyl)-2-(3-nitro-4-methoxy-phenyl)ethene (11a,b). The same procedure used for compound **26a**, after purification on a silica gel column using hexane/ethyl acetate, gave 57 mg (0.15 mmol; 48%) of *Z*-isomer as a yellow oil (**11a**). $R_f = 0.17$ in hex/acetone 8:2. MS (IS): $[M + H]^+ = 382.4$. ^{1}H NMR (200 MHz, $CDCl_3$, δ): 3.76 (s, 6H, 2 × OCH_3), 3.90 (s, 3H, OCH_3), 3.98 (s, 3H, OCH_3), 6.60 (s, 2H, 2 × CHar), 7.02 (d, $J = 8.8$ Hz, 1H, CHar), 7.39 (dd, $J = 8.8$ Hz, $J = 2.2$ Hz, 1H, CHar), 7.90 (s, $J = 2.2$ Hz, 1H, CHar). ^{19}F NMR (282 MHz, $CDCl_3$, δ): −123.7 (d, JFF = 12.2 Hz); −131.7 (d, JFF = 12.2 Hz). A small amount of the *E*-isomer (**11b**) was isolated: ^{1}H NMR (200 MHz, $CDCl_3$, δ): 3.93 (s, 9H, 3 × OCH_3); 4.04 (s, 3H, OCH_3); 7.01 (s, 2H, 2 × CH); 7.20 (d, $J = 8.8$ Hz, 1H, CH); 7.93 (dd, $J = 8.8$ Hz, $J = 2.2$ Hz, 1H, CH); 8.26 (d, $J = 2.2$ Hz, 1H, CH). ^{19}F NMR (282 MHz, $CDCl_3$, δ): −150.1 (d, JFF = 122.1 Hz); −153.2 (d, JFF = 122.1 Hz). Anal. ($C_{18}H_{17}F_2NO_6$) C, H, N.

(*Z*)-1,2-Difluoro-1-(3,4,5-trimethoxyphenyl)-2-(3-amino-4-methoxyphenyl)ethene (14a). To a solution of 40 mg (0.105 mmol) of nitro-stilbene **11a** in AcOH (5 mL), 75 mg (1.15 mmol; 11 equiv) of zinc powder was added; the mixture was stirred at room temperature for 1.5 h. The reaction mixture was filtered over celite and the filtrate evaporated to dryness. The crude product was purified by chromatography on silica gel with CH_2Cl_2, then on preparative HPLC to give 32 mg (0.091 mmol; 87%) of a waxy solid (**14a**). $R_f = 0.31$ in CH_2Cl_2. MS (IS): $[M + H]^+ = 352.3$. ^{1}H NMR (300 MHz, $CDCl_3$, δ): 3.71 (s, 6H, 2 × OCH_3), 3.86 (s, 3H, OCH_3), 3.87 (s, 3H, OCH_3), 6.58 (s, 2H, 2 × CHar), 6.73 (d, 1H, CHar), 6.89 (m, 2H, 2 × CHar). ^{19}F NMR (282 MHz, $CDCl_3$, δ): −125.8 (d, JFF = 15.3 Hz), −131.4 (d, JFF = 15.3 Hz). Anal. ($C_{18}H_{19}F_2NO_4$) C, H, N.

(*E*)-1,2-Difluoro-1-(3,4,5-trimethoxyphenyl)-2-(3-amino-4-methoxyphenyl)ethene (14b). The same protocol applied to the *E*-isomer **11b** gave, with comparable yield, the *E*-isomer of the final aniline (**14b**): $[M + H]^+ = 352.3$. ^{1}H NMR (200 MHz, $CDCl_3$, δ): 3.91 (s, 6H, 2 × OCH_3); 3.92 (s, 3H, OCH_3); 3.94 (s, 3H, OCH_3); 6.90 (d, $J = 8.1$ Hz, 1H, CH); 6.99 (s, 2H, 2 × CH); 7.25 (dd, $J = 8.1$ Hz, $J = 2.2$ Hz, 1H, CH); 7.28 (d, $J = 2.2$ Hz, 1H, CH). ^{19}F NMR (282 MHz, $CDCl_3$, δ): −150.6 (d, JFF = 122.1 Hz); −152.6 (d, JFF = 122.1 Hz). Anal. ($C_{18}H_{19}F_2NO_4$) C, H, N.

1-Bromo-1-(4-methoxyphenyl)-2-fluoro-2-phenyl-ethane (28). To a solution of 231 mg (1.3 mmol; 1.3 equiv) of *N*-bromo-succinimide in 4 mL of dry CH_2Cl_2 and 2 mL of dry Et_2O, previously cooled down to –20 °C, were added 1.25 mL of HF•Pyr. After 10 min at this temperature, 210 mg of (*Z*)-4-methoxy-stilbene (**27**), solubilized in 1 mL of dry Et_2O, were added to the mixture. The reaction was run to completion over one h and the mixture diluted with 20 mL Et_2O and poured into water. The organic phase was neutralized with 5% $NaHCO_3$ (10 mL) and dried over anhydrous sodium sulfate. The crude product was purified by silica gel chromatography using hexane/EtOAc 95:5 to give 196 mg (0.63 mmol; 63%) of a yellow solid. $R_f = 0.55$ (hexane/EtOAc 85:15). $[M + H]^+ = 309.2/311.2$. ^{1}H NMR (200 MHz, $CDCl_3$, δ): 3.85 (s, 3H, OCH_3), 5.15 (dd, $J = 7.5$ Hz, $J = 13.9$ Hz, 1H, CH), 5.85 (dd, $J = 7.5$ Hz, $J = 45.8$ Hz, 1H, CH), 6.90 (d, $J = 8.7$ Hz, 2H, 2 × CHar), 7.25 (d, $J = 8.7$ Hz, 2H, 2 × CHar), 7.35–7.50 (m, 5H, 5 × CHar).

(*E*)-1-(4-Methoxyphenyl)-2-fluoro-2-phenyl-ethene (30). A solution of 25 mg (0.08 mmol) of compound **28** and 14 mL (0.09 mmol; 1.1 equiv) of DBU in 2 mL DMSO was stirred at 80 °C for 3 h. The reaction mixture was poured into water (10 mL), extracted with EtOAc (3 × 15 mL), and dried over anhydrous sodium sulfate. The crude mixture was purified by silica gel chromatography using hexane/EtOAc 97:3 to give 16 mg (0.07 mmol; 88%) of a pale yellow oil. $R_f = 0.67$ (hexane/ EtOAc 9:1). $[M + H]^+ = 229.2$. ^{1}H NMR (200 MHz, $CDCl_3$, δ): 3.70 (s, 3H, OCH_3), 6.25 (d, $J = 21.6$ Hz, 1H, CH), 6.70 (d, $J = 9.2$ Hz, 2H, 2 × CHar), 7.00–7.15 (m, 5H, 5 × CHar), 7.25 (d, $J = 9.2$ Hz, 2H, 2 × CHar).

5-[(*E*/*Z*)-2-Bromo-2-fluoro-vinyl]-2-methoxy-phenol (31a). A solution of $CFBr_3$ (241 μL; 2.4 mmol; 1.2 equiv) and Ph_3P (1.153 g; 4.4 mmol; 2.2 equiv) in 25 mL of CH_2Cl_2 was stirred for 0.5 h in an ice bath; isovanillin (304.4 mg; 2 mmol) was added and the reaction mixture was then kept in an ice bath for 30 min and at room temperature for 2 h until completion. After dilution with CH_2Cl_2 (30 mL) and washing with water (2 × 20 mL), the organic

layer was dried over anhydrous sodium sulfate. Chromatographic separation of the crude product on silica gel with hexane/EtOAc 90:10 gave 150 mg (0.47 mmol; 24%) of an 8:2 *E*/*Z* mixture. R_f = 0.66 in hexane/EtOAc 6:4 for the stereoisomer mixture. A small amount of each of the two geometric isomers (*Z*-isomer as an oil and *E*-isomer as a white solid) was isolated via preparative HPLC to confirm the structure. MS (IS): $[M - H]^-$ = 245.1/247.1. *E*-Isomer: ^{1}H NMR (200 MHz, $CDCl_3$, δ): 3.93 (s, 3H, OCH_3); 5.62 (bs, 1H, OH); 6.59 (d, J = 15.4 Hz, 1H, CH); 6.85 (d, J = 8.1 Hz, 1H, CH); 6.99 (dd, J = 8.1 Hz, J = 2.2 Hz, 1H, CH); 7.16 (d, J = 2.2 Hz, 1H, CH). *Z*-Isomer: ^{1}H NMR (200 MHz, $CDCl_3$, δ): 3.92 (s, 3H, OCH_3); 5.61 (s, 1H, OH); 5.88 (d, J = 32.8 Hz, 1H, CH); 6.82 (d, J = 8.4 Hz, 1H, CH); 6.90 (dd, J = 8.4 Hz, J = 2.2 Hz, 1H, CH); 7.06 (d, J = 2.2 Hz, 1H, CH); mp = 69–71 °C. Anal. ($C_9H_8BrFO_2$) C, H.

5-[(*E*/*Z*)-2-Fluoro-2-(3,4,5-trimethoxy-phenyl)-vinyl]-2-methoxy-phenol (8a,b). A solution of alcohol **31a** (80 mg; 0.32 mmol), 3,4,5-trimethoxybenzenboronic acid (204 mg; 0.96 mmol; 3 equiv), $Pd(Ph_3P)_4$ (20 mg; 0.017 mmol; 0.05 equiv), and 1 mL of 2 M aq Na_2CO_3 in 10 mL toluene was refluxed overnight until completion. After the addition of anhydrous sodium sulfate, the reaction mixture was passed through a short silica pad to remove catalyst. Chromatography of the crude product on silica gel with hexane/EtOAc 85:15 to 8:2 gave 70 mg (0.21 mmol; 66%) of a 2.6:1 *Z*/*E* mixture (by ^{1}H NMR), which could not be separated even by preparative HPLC but only after derivatization as silyl ether. Deprotection of the silyl derivative (**33**) with TBAF (see compound **7**) gave the final product as a colorless oil. R_f = 0.13 in hexane/EtOAc 8:2. MS (IS): $[M - H]^-$ = 333.2. *E*-Isomer (**8a**): ^{1}H NMR (200 MHz, $CDCl_3$, δ): 3.73 (s, 6H, 2 × OCH_3); 3.89 (s, 6H, 2 × OCH_3); 5.55 (s, 1H, OH); 6.36 (d, J = 22 Hz, 1H, CH); 6.70–6.75 (m, 4H, 4 × CH); 6.85 (d, J = 1.5 Hz, 1H, CH). *Z*-Isomer (**8b**): ^{1}H NMR (200 MHz, $CDCl_3$, δ): 3.90 (s, 6H, 2 × OCH_3); 3.94 (s, 6H, 3 × OCH_3); 5.64 (s, 1H, OH); 6.14 (d, J = 39.6 Hz, 1H, CH); 6.85 (s, 2H, 2 × CH); 6.87 (d, J = 8.4 Hz, 1H, CH); 7.14 (dd, J = 8.4 Hz, J = 1.8 Hz, 1H, CH); 7.31 (d, J = 1.8 Hz, 1H, CH). Anal. ($C_{18}H_{19}FO_5$) C, H.

4-[(*E*/*Z*)-2-Bromo-2-fluoro-vinyl]-1-methoxy-2-nitro-benzene (31b). A solution of $CFBr_3$ (241 μL; 2.4 mmol; 1.2 equiv) and Ph_3P (1.153 g; 4.4 mmol; 2.2 equiv) in 25 mL of CH_2Cl_2 was stirred for 0.5 h in an ice bath; 3-nitro-4-methoxybenzaldehyde (362.4 mg; 2 mmol) was added and the reaction mixture was kept in an ice bath for 30 min and at room temperature for 2 h until completion. After dilution with CH_2Cl_2 (30 mL) and washing with water (2 × 20 mL), the organic layer was dried over anhydrous sodium sulfate. Chromatographic separation of the crude product on silica gel with hexane/EtOAc 90:10 gave 130 mg (0.47 mmol; 24%) of a 65.8:34.2 *E*/*Z* mixture. Irradiation of the mixture (at a concentration of 1 mg/mL in CH_3CN) with a 160 W lamp at 366 nm led to a 45.4:54.6 *E*/*Z* ratio. R_f = 0.61 in hexane/EtOAc 7:3. A small amount of each of the two geometric isomers was isolated as yellow oils via preparative HPLC to confirm the structure. MS (IS): $[MH]^+$ = 276.1/278.1 $[M + Na]^+$ = 298.1/300.1. *Z*-Isomer: ^{1}H NMR (200 MHz, $CDCl_3$, δ): 4.00 (s, 3H, OCH_3); 6.63 (d, J = 14.3 Hz, 1H, CH); 7.11 (d, J = 8.8 Hz, 1H, CH); 7.67 (dd, J = 8.8 Hz, J = 2.2 Hz, 1H, CH); 8.04 (d, J = 2.2 Hz, 1H, CH). *E*-Isomer: ^{1}H NMR (200 MHz, $CDCl_3$, δ): 4.00 (s, 3H, OCH_3); 5.96 (d, J = 31.9 Hz, 1H, CH); 7.08 (d, J = 8.8 Hz, 1H, CH); 7.60 (dd, J = 8.8 Hz, J = 2.2 Hz, 1H, CH); 7.90 (d, J = 2.2 Hz, 1H, CH). Anal. ($C_9H_7BrFNO_3$) C, H, N.

5-[(*E*/*Z*)-1-Fluoro-2-(4-methoxy-3-nitro-phenyl)-vinyl]-1,2,3-trimethoxy-benzene (12a,b). A solution of alcohol **31b** (104 mg; 0.38 mmol), 3,4,5-trimethoxybenzenboronic acid (242 mg; 1.14 mmol; 3 equiv), $Pd(Ph_3P)_4$ (23 mg; 0.02 mmol; 0.05 equiv), and 1 mL of 2 M aq Na_2CO_3 in 10 mL toluene was refluxed overnight until completion. After addition of anhydrous sodium sulfate, the reaction mixture was passed through a short silica pad to remove catalyst. Chromatography of the crude product on silica gel with hexane/EtOAc 90:10 to 85:15 gave 25 mg (0.07 mmol; 18%) of *E*-isomer and 23 mg (0.06 mmol; 16%) of *Z*-isomer, both isomers obtained as yellow solids. R_f = 0.39 in hexane/EtOAc 7:3 for *E*-isomer, and R_f = 0.26 for *Z*-isomer. MS (IS): $[M + Na]^+$ = 386.3. *E*-Isomer (**12a**): ^{1}H NMR (200 MHz, $CDCl_3$, δ): 3.74 (s, 6H, 2 × OCH_3); 3.89 (s, 3H, OCH_3); 3.95 (s, 3H, OCH_3); 6.34 (d, J = 20.5 Hz, 1H, CH); 6.66 (s, 2H, 2 × CH); 6.97 (d, J = 8.8 Hz, 1H, CH); 7.35 (dd, J = 8.8 Hz, J = 2.2 Hz, 1H, CH); 7.72 (d, J = 2.2 Hz, 1H, CH); mp = 124–127 °C. *Z*-Isomer (**12b**): ^{1}H NMR (200 MHz, $CDCl_3$, δ): 3.91 (s, 3H, OCH_3); 3.94 (s, 6H, 2 × OCH_3); 4.00 (s, 3H, OCH_3); 6.18 (d, J = 38.5 Hz, 1H, CH); 6.85 (s, 2H, 2 × CH); 7.11 (d, J = 8.8 Hz, 1H, CH); 7.81 (dd, J = 8.8 Hz, J = 2.2 Hz, 1H, CH); 8.13 (d, J = 2.2 Hz, 1H, CH). T_{dec} = 220 °C. Anal. ($C_{18}H_{18}FNO_6$) C, H, N.

5-[(*E*)-2-Fluoro-2-(3,4,5-trimethoxy-phenyl)-vinyl]-2-methoxy-phenylamine (15a). Zinc powder (40 mg; 0.6 mmol; 20 equiv) was added at room temperature to a solution of nitro stilbene **12a** (12 mg; 0.03 mmol) in 2 mL of acetic acid; the reaction mixture was stirred overnight at RT. After dilution with EtOAc (10 mL), the organic layer was washed with 2 N aq NaOH (2 × 5 mL), and the crude product was purified by chromatography on silica gel with hexane/EtOAc 7:3 to give 9 mg (0.027 mmol; 89%) of a pale yellow oil. R_f = 0.37 in hexane/EtOAc 7:3. MS (IS): $[M + H]^+$ = 334.2, $[M + Na]^+$ = 356.2. ^{1}H NMR (200 MHz, $CDCl_3$, δ): 3.73 (s, 6H, 2 × OCH_3); 3.85 (s, 3H, OCH_3); 3.88 (s, 3H, OCH_3); 6.35 (d, J = 21.9 Hz, 1H, CH); 6.67–6.73 (m, 5H, 5 × CH). Anal. ($C_{18}H_{20}FNO_4$) C, H, N.

5-[(*Z*)-2-Fluoro-2-(3,4,5-trimethoxy-phenyl)-vinyl]-2-methoxy-phenylamine (15b). The same protocol as **15a** gave **15b** as a pale yellow oil. R_f = 0.29 in hexane/EtOAc 7:3. MS (IS): $[M + H]^+$ = 334.2, $[M + Na]^+$ = 356.2. ^{1}H NMR (200 MHz, $CDCl_3$, δ): 3.90 (s, 3H, OCH_3); 3.91 (s, 3H, OCH_3); 3.93 (s, 6H, 2 × OCH_3); 6.13 (d, J = 39.6 Hz, 1H, CH); 6.83 (s, 2H, 2 × CH); 6.84 (d, J = 8.4 Hz, 1H, CH); 7.11 (dd, J = 8.4 Hz, J = 2.2 Hz, 1H, CH); 7.25 (d, J = 2.2 Hz, 1H, CH). Anal. ($C_{18}H_{20}FNO_4$) C, H, N.

2,2,2-Tribromo-1-[3-(*tert*-butyl-dimethyl-silanyloxy)-4-methoxyphenyl]-ethanol (34). To a solution of **22a** (2.66 g; 10 mmol) and CBr_4 (5.31 g; 16 mmol; 1.6 equiv) in 50 mL of Et_2O/THF 1:1, previously cooled down to –129 °C, a 1.6 M BuLi solution (9 mL; 14 mmol; 1.4 equiv) was added dropwise in an inert atmosphere. The reaction mixture was allowed to warm up to –70 °C until completion; the solution was then diluted with EtOAc (40 mL) and washed with NH_4Cl saturated solution (40 mL). The crude product was purified by chromatography on silica gel with hexane/EtOAc 9:1 to give 3.3 g (6.4 mmol; 40%) of product as an orange oil. R_f = 0.42 in hexane/EtOAc 9:1. MS (IS): $[M + Na]^+$ = 538.9/540.9/542.9/544.9. ^{1}H NMR (200 MHz, $CDCl_3$, δ): 0.18 (s, 6H, 2 × CH_3); 1.02 (s, 9H, 3 × CH_3); 3.50 (d, J = 3.7 Hz, 1H, OH); 3.84 (s, 3H, OCH_3); 5.09 (d, J = 3.7 Hz, 1H, CH); 6.85 (d, J = 8.4 Hz, 1H, CH); 7.22 (d, J = 2.2 Hz, 1H, CH); 7.27 (dd, J = 8.4 Hz, J = 2.2 Hz, 1H, CH). Anal. ($C_{15}H_{23}Br_3O_3Si$) C, H.

***tert*-Butyl-[2-methoxy-5-(2,2,2-tribromo-1-fluoro-ethyl)-phenoxy]-dimethyl-silane (35).** (Diethylamino)sulfur trifluoride 0.65 mL (5 mmol; 1.6 equiv) in 10 mL of CH_2Cl_2 was added to a solution of 1.6 g (3.1 mmol) alcohol **34** in 10 mL CH_2Cl_2 at −78 °C. The reaction mixture was allowed to warm up to 0 °C over a period of 2 h, quenched with 25 mL of $NaHCO_3$ saturated solution, and diluted with 20 mL of CH_2Cl_2. The organic phase was dried over anhydrous sodium sulfate and purified by chromatography on silica gel using hexane/ethyl acetate 95:5 to give 1.213 g (2.32 mmol; 74.8%) of a yellow oil. R_f = 0.60 (hex/AcOEt 9:1). MS (IS): $[M + Na]^+$ = 540.8/542.8/544.9/546.9. ^{1}H NMR (200 MHz, $CDCl_3$, δ): 0.20 (s, 6H, 2 × CH_3); 1.03 (s, 9H, 3 × CH_3); 3.87 (s, 3H, OCH_3); 5.72 (d, J = 42.9 Hz, 1H, CH); 6.90 (d, J = 8.4 Hz, 1H, CH); 7.23 (d, J = 2.2 Hz, 1H, CH); 7.28 (dd, J = 8.4 Hz, J = 2.2 Hz, 1H, CH). Anal. ($C_{15}H_{22}Br_3FO_2Si$) C, H.

***tert*-Butyl-[5-(2,2-dibromo-1-fluoro-vinyl)-2-methoxy-phenoxy]-dimethyl-silane (36).** DBU (0.411 mL; 2.7 mmol; 1.5 equiv) was added to a solution of 940 mg (1.8 mmol) of **35** in 10 mL of CH_2Cl_2 at room temperature, and the reaction mixture stirred overnight at RT. The solution was diluted with CH_2Cl_2 (30 mL) and washed with water (2 × 20 mL). The crude product was purified by silica gel chromatography with hexane/EtOAc 98:2 to give 658 mg (1.49 mmol; 83%) of a pale yellow oil. R_f = 0.4 in hexane/EtOAc 96:4.

MS (IS): $[M + Na]^+ = 461.0/463.0/464.0$. ^1H NMR (200 MHz, $CDCl_3$, δ): 0.20 (s, 6H, 2 × CH_3); 1.04 (s, 9H, 3 × CH_3); 3.86 (s, 3H, OCH_3); 6.89 (d, $J = 8.4$ Hz, 1H, CH); 7.24 (d, $J = 2.2$ Hz, 1H, CH); 7.31 (dd, $J = 8.4$ Hz, $J = 2.2$ Hz, 1H, CH). Anal. ($C_{15}H_{21}Br_2FO_2Si$) C, H.

{5-[(*Z*/*E*)-2-Bromo-1-fluoro-2-(3,4,5-trimethoxy-phenyl)-vinyl]-2-methoxy-phenoxy}-*tert*-butyl-dimethyl-silane (37). A solution of **36** (232 mg; 0.53 mmol), 3,4,5-trimethoxybenzenboronic acid (330 mg; 1.56 mmol; 3 equiv), $Pd(Ph_3P)_4$ (30 mg; 0.026 mmol; 0.05 equiv), and 2 mL of 2 M aq Na_2CO_3 in 10 mL of toluene was refluxed overnight until completion. After addition of anhydrous sodium sulfate, the reaction mixture was passed through a short silica pad to remove catalyst. Chromatography of the crude product on silica gel with hexane/EtOAc 95: 5 to 8:2 gave 87 mg (0.17 mmol; 32%) of the *Z*-isomer (by ^1H NMR NOE) and 12 mg (0.023 mmol; 4%) of the *E*-isomer; both isomers obtained as pale yellow oils. $R_f = 0.3$ in hexane/EtOAc 9:1 for *Z*-isomer. $R_f = 0.35$ in hexane/EtOAc 9:1 for *E*-isomer. MS (IS): $[M + Na]^+ = 549.3/551.3$. *Z*-Isomer: ^1H NMR (200 MHz, $CDCl_3$, δ): 0.02 (s, 6H 2 × CH_3); 0.92 (s, 9H, 3 × CH_3); 3.75 (s, 6H, 2 × OCH_3); 3.79 (s, 3H, OCH_3); 3.86 (s, 3H, OCH_3); 6.57 (s, 2H, 2 × CH); 6.69 (d, $J = 2.2$ Hz, 1H, CH); 6.72 (d, $J = 9.5$ Hz, 1H, CH); 6.92 (dd, $J = 8.5$ Hz, $J = 2.2$ Hz, 1H, CH). *E*-Isomer: ^1H NMR (200 MHz, $CDCl_3$, δ): 0.17 (s, 6H, 2 × CH_3); 1.00(s, 9H, 3 × CH_3); 3.85 (s, 3H, OCH_3); 3.87 (s, 3H, OCH_3); 3.88 (s, 6H, 2 × OCH_3); 6.82 (s, 2H, 2 × CH); 6.87 (d, $J = 8.4$ Hz, 1H, CH); 7.32 (d, $J = 2.2$ Hz, 1H, CH); 7.37 (dd, $J = 8.4$ Hz, $J = 2.2$ Hz, 1H, CH). Anal. ($C_{24}H_{32}BrFO_5Si$) C, H.

***tert*-Butyl-{5-[(*E*/*Z*)-1-fluoro-2-(3,4,5-trimethoxy-phenyl)-vinyl]-2-methoxy-phenoxy}-dimethyl-silane (38a,b).** Both geometric isomers of **38** were obtained by two different approaches. Via **37**: Tributyltin hydride (82 μL; 0.28 mmol; 4.4 equiv) and AIBN (5 mg; 0.03; 0.47 equiv) were added to a solution of **37** (34 mg; 0.064 mmol) in 3 mL of 1,2-dichloroethane and refluxed. After 16 h, another 82 μL of Bu_3SnH and 5 mg of AIBN were necessary to drive the reaction to completion. After cooling to room temperature, the reaction mixture was diluted with CH_2Cl_2 (20 mL), and washed with water (2 × 10 mL). Chromatography of the crude product on silica gel with hexane/EtOAc 85:15 gave 23 mg (0.051 mmol; 80%) of a pale yellow oil.

Via **39**: (a) Debromination. Tributyltin hydride (358 μL; 1.23 mmol; 4.4 equiv) and AIBN (23 mg; 0.14; 0.5 equiv) were added to a solution of **36** (123 mg; 0.28 mmol) in 3 mL of 1,2-dichloroethane and refluxed. After 16 h, another 358 μL of Bu_3SnH and 23 mg of AIBN were necessary to drive the reaction to completion. After cooling to room temperature, the reaction mixture was diluted with CH_2Cl_2 (20 mL) and washed with water (2 × 10 mL). Chromatography of the crude product on silica gel with hexane/EtOAc 98:2 gave 62 mg (0.25 mmol; 89%) of product as a mixture of the two isomers *Z*/*E* (1:2.2), whose ratio was determined both by ^1H NMR and by HPLC. (b) Suzuki reaction. A solution of debrominated product obtained in the previous step (62 mg; 0.25 mmol), 3,4,5-trimethoxybenzenboronic acid (159 mg; 0.75 mmol; 3 equiv), $Pd(Ph_3P)_4$ (14 mg; 0.012 mmol; 0.05 equiv), and 1 mL of 2 M aq Na_2CO_3 in 10 mL toluene was refluxed overnight until completion. After addition of anhydrous sodium sulfate, the reaction mixture was passed through a short silica pad to remove catalyst. Chromatography of the crude product on silica gel with hexane/EtOAc 95:5 to 8:2 gave 13 mg (0.029 mmol; 12%) of the *Z*-isomer and 11 mg (0.025 mmol; 10%) of the *E*-isomer. MS (IS): $[M + Na]^+ = 449.3/451.3$. *E*-Isomer (**38a**): $R_f = 0.7$ in hexane/EtOAc 9:1. ^1H NMR (200 MHz, $CDCl_3$, δ): 0.09 (s, 6H 2 × CH_3); 0.95 (s, 9H, 3 × CH_3); 3.71 (s, 6H, 2 × OCH_3); 3.83 (s, 3H, OCH_3); 3.84 (s, 3H, OCH_3); 6.31 (d, $J = 20.9$ Hz, 1H, CH); 6.42 (s, 2H, 2 × CH); 6.80 (d, $J = 8.4$ Hz, 1H, CH); 6.94 (d, $J = 2.2$ Hz, 1H, CH); 7.081 (dd, $J = 8.4$ Hz, $J = 2.2$ Hz, 1H, CH). *Z*-Isomer (**38b**): $R_f = 0.6$ in hexane/EtOAc 9:1. ^1H NMR (200 MHz, $CDCl_3$, δ): 0.21 (s, 6H, 2 × CH_3); 1.04 (s, 9H, 3 × CH_3); 3.87 (s, 3H, OCH_3); 3.89 (s, 3H, OCH_3); 3.92 (s, 6H, 2 × OCH_3); 6.08 (d, $J = 39.2$ Hz, 1H, CH); 6.88 (d, $J = 8.4$ Hz, 1H, CH); 6.89 (s, 2H, 2 × CH); 7.12 (d, $J = 2.2$ Hz, 1H, CH); 7.23 (dd, $J = 8.4$ Hz, $J = 2.2$ Hz, 1H, CH). Anal. ($C_{24}H_{33}FO_5Si$) C, H.

5-[(*E*)-1-Fluoro-2-(3,4,5-trimethoxy-phenyl)-vinyl]-2-methoxy-phenol (9a). A solution of **38** (23 mg; 0.051 mmol) was dissolved in 2 mL of THF, and 100 μL (0.100 mmol; 2 equiv) of 1 M TBAF in THF were added. The reaction was run to completion in 1 h. After dilution with EtOAc (5 mL) and washing with H_2O (5 mL), the crude product was chromatographed on silica gel with hexane/EtOAc 7:3 to give 12 mg (0.036; 71%) of a waxy white solid. $R_f = 0.20$ in hexane/EtOAc 8:2. MS (IS): $[M - H]^- = 333.1$. ^1H NMR (300 MHz, $CDCl_3$ δ): 3.71 (s, 6H, 2 × OCH_3); 3.85 (s, 3H, OCH_3); 3.92 (s, 3H, OCH_3); 5.61 (s, 1H, OH); 6.43 (s, 2H, 2 × CH); 6.80 (dd, $J = 8.4$ Hz, $J = 0.7$ Hz, 1H, CH); 7.01 (dq, $J = 8.4$ Hz, $J = 1.8$ Hz, $J = 0.7$ Hz, 1H, CH); 7.10 (d, $J = 1.8$ Hz, 1H, CH). Anal. ($C_{18}H_{19}FO_5$) C, H.

5-[(*Z*)-1-Fluoro-2-(3,4,5-trimethoxy-phenyl)-vinyl]-2-methoxy-phenol (9b). Analogous deprotection of the *Z*-isomer of **38** gave **9b**: ^1H NMR (300 MHz, $CDCl_3$ δ): 3.92 (s, 6H, 2 × OCH_3); 5.67 (bs, 1H, OH); 6.12 (d, $J = 39.2$ Hz, 1H, CH); 6.88 (s, 2H, 2 × CH); 6.89 (d, $J = 8.1$ Hz, 1H, CH); 7.18 (dd, $J = 8.06$ Hz, $J = 2.2$ Hz, 1H, CH); 7.21 (d, $J = 2.2$ Hz, CH). Anal. ($C_{18}H_{19}FO_5$) C, H.

5-[(*Z*)-2-Bromo-1-fluoro-2-(3,4,5-trimethoxy-phenyl)-vinyl]-2-methoxy-phenol (10). A solution of **37** (*Z*-isomer) (20 mg; 0.038 mmol) was dissolved in 2 mL THF, 76 μL (0.076 mmol; 2 equiv) of 1 M TBAF in THF were added. The reaction was run to completion in 1 h. After dilution with EtOAc (5 mL) and washing with H_2O (5 mL), the crude product was chromatographed on silica gel with hexane/EtOAc 7:3 to give 14 mg (0.034 mmol; 89%) of a white solid. $R_f = 0.11$ in hexane/EtOAc 8:2. MS (IS): $[M - H]^- = 411.1/413.1$, $[M + Na]^+ = 435.1/437.1$. ^1H NMR (300 MHz, $CDCl_3$, δ): 3.76 (s, 6H, 2 × OCH_3); 3.88 (s, 6H, 2 × OCH_3); 5.56 (s, 1H, OH); 6.57 (s, 2H, 2 × CH); 6.67 (d, $J = 8.8$ Hz, 1H, CH); 6.73 (dd, $J = 8.8$ Hz, $J = 1.8$ Hz, 1H, CH); mp = 104–107 °C. Anal. ($C_{18}H_{18}BrFO_5$) C, H.

5-[(*Z*/*E*)-2-Bromo-2-fluoro-vinyl]-1,2,3-trimethoxy-benzene (41a,b). A solution of $CFBr_3$ (600 μL; 6 mmol; 1.2 equiv) and Ph_3P (5.8 g; 22 mmol; 4.4 equiv) in 40 mL of CH_2Cl_2 was stirred for 0.5 h in an ice bath; 3,4,5-trimethoxybenzaldheyde (**40**; 980 mg; 5 mmol) was added and the reaction mixture then kept in an ice bath for 30 min and at room temperature for 2 h until completion. After dilution with CH_2Cl_2 (30 mL) and washing with water (2 × 20 mL), the organic layer was dried over anhydrous sodium sulfate. Chromatographic separation of the crude product on silica gel with hexane/EtOAc 90:10 gave 600 mg (2.1 mmol; 42%) of a 1:1 *E*/*Z* mixture. $R_f = 0.23$ in hexane/EtOAc 9:1. A small amount of each of the two geometric isomers was isolated via preparative HPLC, as pale yellow oils, to confirm the structure. MS (IS): $[MH]^+ = 291.1/294.0$. *Z*-Isomer (**41a**): ^1H NMR (200 MHz, $CDCl_3$, δ): 3.88 (s, 9H, 3 × OCH_3); 6.62 (d, $J = 15.4$ Hz, 1H, CH); 6.75 (s, 2H, 2 × CH). *E*-Isomer (**41b**): ^1H NMR (200 MHz, $CDCl_3$, δ): 3.87 (s, 9H, 3 × OCH_3); 5.93 (d, $J = 32.2$ Hz, 1H, CH); 6.65 (s, 2H, 2 × CH). Anal. ($C_{11}H_{12}BrFO_3$) C, H.

5-[(*E*/*Z*)-2-Fluoro-2-(4-methoxy-3-nitrophenyl)-vinyl]-1,2,3-trimethoxy-benzene (13a,b). A solution of stirene **41** (102 mg; 0.35 mmol), of 3-nitro-4-methoxyphenylboronic acid (234 mg; 1.19 mmol; 3.4 equiv), $Pd(Ph_3P)_4$ (21 mg; 0.018 mmol; 0.05 equiv), and 1 mL of 2 M aq Na_2CO_3 in 10 mL toluene was refluxed overnight until completion. After addition of anhydrous sodium sulfate, the reaction mixture was passed through a short silica pad to remove catalyst. Chromatography of the crude product on silica gel with hexane/EtOAc 90:10 to 85:15 gave 35 mg (0.097 mmol; 27%) of *E*-isomer as a yellow oil and 373 mg (0.10 mmol; 29%) of *Z*-isomer as a yellow solid. $R_f = 0.36$ in hexane/EtOAc 7:3 for *E*-isomer and $R_f = 0.23$ for *Z*-isomer. MS (IS): $[M + Na]^+ = 386.3$. *E*-Isomer (**13a**): ^1H NMR (200 MHz, $CDCl_3$, δ): 3.74 (s, 6H, 2 × OCH_3); 3.86 (s, 3H, OCH_3); 3.98 (s, 3H, OCH_3); 6.42 (s, 2H, 2 × CH); 6.47 (d, $J = 20.2$ Hz, 1H, CH); 7.01 (d, $J = 9.2$ Hz, 1H, CH); 7.59 (dd, $J = 9.2$ Hz, $J = 2.2$ Hz, 1H, CH); 8.00 (d, $J = 2.2$ Hz, 1H, CH). *Z*-Isomer (**13b**): ^1H NMR (200 MHz, $CDCl_3$, δ): 3.90 (s, 3H, OCH_3); 3.92 (s, 6H, 2 × OCH_3); 4.03 (s, 3H, OCH_3); 6.22 (d, $J = 38.8$ Hz, 1H, CH); 6.90 (s, 2H, 2 × CH); 7.15 (d, *J*

= 9.2 Hz, 1H, CH); 7.80 (dd, J = 9.2 Hz, J = 2.2 Hz, 1H, CH); 8.12 (d, J = 2.2 Hz, 1H, CH); mp = 138–141 °C. Anal. ($C_{18}H_{18}FNO_6$) C, H, N.

5-[(*E*)-1-Fluoro-2-(3,4,5-trimethoxy-phenyl)-vinyl]-2-methoxy-phenylamine (16a). Zinc in powder (97 mg; 1.48 mmol; 20 eq.) was added, at room temperature, to a solution of stilbene **13a** (27 mg; 0.074 mmol) in 2 mL of acetic acid; the reaction mixture was stirred overnight at RT. After dilution with EtOAc (10 mL), the organic layer was washed with 2 N aq NaOH (2 × 5 mL), and the crude product was purified by chromatography on silica gel with hexane/EtOAc 7:3 to give 20 mg (0.060 mmol; 81%) of a pale yellow oil (**16a**). R_f = 0.49 in hexane/EtOAc 6:4. MS (IS): $[M + Na]^+$ = 356.2. ^{1}H NMR (200 MHz, $CDCl_3$, δ): 3.71 (s, 6H, 2 × OCH_3); 3.85 (s, 3H, OCH_3); 3.88 (s, 3H, OCH_3); 6.28 (d, J = 21.6 Hz, 1H, CH); 6.44 (s, 2H, 2 × CH); 6.74 (d, J = 9.2 Hz, 1H, CH); 6.91–6.94 (m, 2H, 2 × CH). Anal. ($C_{18}H_{20}FNO_4$) C, H, N.

5-[(*Z*)-1-Fluoro-2-(3,4,5-trimethoxy-phenyl)-vinyl]-2-methoxy-phenylamine (16b). The above-described synthetic procedure gave the *Z*-isomer **16b** with 77% yield as a pale yellow oil. R_f = 0.50 in hexane/EtOAc 6:4. MS (IS): $[M + Na]^+$= 356.2. ^{1}H NMR (200 MHz, $CDCl_3$, δ): 3.89 (s, 3H, OCH_3); 3.91 (s, 6H, 2 × OCH_3); 3.92 (s, 3H, OCH_3); 6.10 (d, J = 39.2 Hz, 1H, CH); 6.85 (d, J = 10.6 Hz, 1H, CH); 6.88 (s, 2H, 2 × CH); 7.107–7.142 (m, 2H, 2 × CH). Anal. ($C_{18}H_{20}FNO_4$) C, H, N.

6-[(*E*)-2-Fluoro-2-(3,4,5-trimethoxy-phenyl)-vinyl]-benzo-[b]thiophen-4-ol (18a). The procedure used for compound **31a** gave intermediate **42a**, which without further purification underwent Suzuki coupling to give, after preparative HPLC purification with CH_3CN/H_2O 60:40, 9 mg (0.025 mmol; 18% in two steps) of the final compound **44a** as a yellow solid. R_f = 0.50 in hexane/EtOAc 7:3. $[M - H]^-$ = 359.3. ^{1}H NMR (200 MHz, $CDCl_3$, δ): 3.66 (s, 6H, 2 × OCH_3); 3.,88 (s, 3H, OCH_3); 6.49 (d, J = 21.6 Hz, 1H, CH); 6.61 (s, 1H,CH); 6.71 (s, 2H, 2 × CH); 7.34 (d, J = 5.4 Hz, 1H, CH); 7.36 (s, 1H, CH); 7.42 (d, J = 5.4 MHz, 1H, CH); mp = 158–161 °C. Anal. ($C_{19}H_{17}FO_4S$) C, H, S.

6-[(*Z*)-2-Fluoro-2-(3,4,5-trimethoxy-phenyl)-vinyl]-benzo-[*b*]thiophen-4-ol (18b). Analogous procedure gave the *Z*-isomer as yellow solid: R_f = 0.33 in Hexane/EtOAc 7:3. ^{1}H NMR (200 MHz, $CDCl_3$, δ): 3.92 (s, 3H, OCH_3); 3.95 (s, 6H, 2 × OCH_3); 6.28 (d, J = 39.2 Hz, 1H, CH); 6.88 (s, 2H, 2 × CH); 7.12 (s, 1H, CH); 7.39 (d, J = 5.5 Hz, 1H, CH); 7.47 (d, J = 5.5 Hz, 1H, CH); 7.72 (s, 1H, CH); mp = 134–137 °C. Anal. ($C_{19}H_{17}FO_4S$) C, H, S.

6-[(*E*)-2-Fluoro-2-(3,4,5-trimethoxy-phenyl)-vinyl]-benzofuran-4-ol (19a). The procedure applied for **18** gave compound **19a** in a 22% yield (two steps) as a pale yellow oil. R_f = 0.37 in hexane/EtOAc 7:3. $[M - H]^-$ = 343.2. ^{1}H NMR (200 MHz, $CDCl_3$, δ): 3.68 (s, 6H, 2 × OCH_3); 3.,89 (s, 3H, OCH_3); 6.49 (d, J = 21.5 Hz, 1H, CH); 6.53 (bs, 1H, CH); 6.70 (s, 2H, 2 × CH); 6.81 (dd, J = 2.2 Hz, J = 0.7 Hz, 1H, CH); 7.03 (bs, 1H, CH); 7.54 (d, J = 2.2 Hz, 1H, CH). Anal. ($C_{19}H_{17}FO_5$) C, H.

6-[(*Z*)-2-Fluoro-2-(3,4,5-trimethoxy-phenyl)-vinyl]-benzofuran-4-ol (19b). Analogous procedure of **19a** gave the *Z*-isomer (**19b**) as a yellow oil: R_f = 0.23 in hexane/EtOAc 7:3. ^{1}H NMR (200 MHz, $CDCl_3$, δ): 3.91 (s, 3H, OCH_3); 3.95 (s, 6H, 2 × OCH_3); 6.26 (d, J = 38.8 Hz, 1H, CH); 6.86 (d, J = 2.2 Hz, 1H, CH); 6.88 (s, 2H, 2 × CH); 6.99 (s, 1H, CH); 7.44 (s, 1H, CH); 7.60 (d, J = 2.2 Hz, 1H, CH). Anal. ($C_{19}H_{17}FO_5$) C, H.

5-[(*E*/*Z*)-2-Fluoro-2-(3-fluoro-4-methoxy-phenyl)-vinyl]-1,2,3-trimethoxy-benzene (17a,b). The same procedure used for compound **13** gave, after purification by chromatography on silica gel with hexane/EtOAc 9:1, the final product in a 40% yield (R_f = 0.38 in hexane/EtOAc 8:2) together with its *Z*-isomer (22%; R_f = 0.30 in hexane/EtOAc 8:2). *E*-Isomer **17a**: $[M + H]^+$ = 337.2, $[M + Na]^+$ = 359.2. ^{1}H NMR (200 MHz, $CDCl_3$, δ): 3.71 (s, 6H, 2 × OCH_3); 3.85 (s, 3H, OCH_3); 3.90 (s, 3H, OCH_3); 6.36 (d, J = 22.3 Hz); 6.41 (s, 2H, 2 × CH); 6.89 (t, J = 8.5 Hz, 1H, CH); 7.19–7.28 (m, 2H, 2 × CH); white solid, mp = 101–104 °C. *Z*-Isomer **17b**: ^{1}H NMR (200 MHz, $CDCl_3$, δ): 3.89 (s, 3H, OCH_3); 3.91 (s, 6H, 2 × OCH_3); 3.94 (s, 3H, OCH_3); 6.13 (d, J = 39.2 Hz, 1H, CH); 6.88 (s, 2H, 2 × CH); 6.99 (t, J = 8.4 Hz, 1H, CH); 7.32–7.40 (m, 2H, 2CH). Anal. ($C_{18}H_{18}F_2O_4$) C, H.

(*Z*)-1,2-Difluoro-1-(3,4,5-trimethoxyphenyl)-2-(3-hydroxy-4-methoxyphenyl)ethene *O*-Disodium Phosphate (43). According to the cited three-step protocol,[5,30] we obtained the disodium phosphate prodrug of **7** as a white solid: $[M - 2Na + H]^-$ = 431.2 ^{1}H NMR (300 MHz, D_2O, δ): 3.55 (s, 6H, 2 × OCH_3); 3.63 (s, 3H, OCH_3); 3.70 (s, 3H, OCH_3); 6.59 (s, 2H, 2 × CH); 6.72 (d, J = 8.1 Hz, 1H, CH); 6.78 (d, J = 8.1 Hz, 1H, CH); 7.48 (s, 1H, CH). Anal. ($C_{18}H_{17}F_2O_8PNa_2$) C, H.

Biology

Cell Culture. Primary cultures of bovine microvascular endothelial cells (BMEC) were obtained from bovine adrenal glands as described by Folkman.[45] BMEC were maintained in DMEM, supplemented with 20% fetal calf serum (FCS), 50 units/mL heparin (Sigma, St. Louis, MO), 50 μg/mL bovine brain extract, and 100 units/mL gentamycin.

NCI-H460 human nonsmall cell lung carcinoma and HT29 colon carcinoma were purchased from ATCC and cultured according to manufacturer's instructions.

Tubulin Polymerization Assay. The tubulin polymerization test was performed by CytoDINAMIX ScreenTM (Cytoskeleton Inc., Denver, CO). A total of 100 μL of 3 mg/mL HTS tubulin in G-PEM buffer plus 5% glycerol at 4 °C were pipetted into wells of the 96-well plate and incubated at 37 °C in presence or absence of single compounds. Tubulin polymerization was detected by measuring the absorbance of the solution (340 nm) for 60 min. Because the amount of tubulin polymerized is directly proportional to the AUC (area under the curve), we used AUC to determine the concentration that inhibited tubulin polymerization by 50% (IC_{50}). The AUC of the untreated control was set to 100% polymerization (maximal attainable), and the IC_{50} was calculated by nonlinear regression.

Cytotoxicity Assay. To test the effect of the drugs on cell growth, the above cell lines were resuspended at different concentrations in 200 μL of appropriate growth medium and seeded in 96-well plates. A total of 24 h after plating, scalar concentrations of each drug were added to the cells. The drugs were removed after 24 h and, after an additional 48 h of recovery, the number of surviving cells was determined by staining with sulforhodamine B test as previously described.[46] Optical density was measured at 564 nm. Results, expressed as concentrations that inhibit 50% of cell growth (IC_{50}), were calculated by the ALLFIT program.

Flow Cytometry. NCI-H460 cells were seeded in 100 mm plastic dishes in RPMI-1640 complete medium, allowed to adhere, and exposed for 24 h to the various molecules (IC_{80} dose). The cells were then harvested with trypsin/EDTA, pooled with the respective supernatant, and fixed in ice-cold 70% ethanol at 4 °C. On the day of analysis, ethanol was removed by centrifugation, and cells were rinsed twice with PBS and treated with RNase (75 KU/mL) for 30 min at 37 °C. Propidium iodide (PI) was finally added (50 μg/mL) to stain cellular DNA, and samples (2 × 10^4 cells) were processed on a FACScan flow cytometer (Becton Dickinson) to assess cell cycle distribution and apoptosis. Apoptosis was evaluated by measuring the percentage of cells with hypodiploid DNA content (sub-$G_{1/0}$ population) with CELLQuest software, while cell cycle analysis was performed with ModFit software.

Immunofluorescence. For tubulin immunostaining, the cells, cultured on gelatin-coated coverslips, were treated with the compounds at concentrations near their respective IC_{80}values. After 24 h, the cells were washed with PBS and then fixed in cold methanol for 5 min and acetone for 1 min. Next, the fixed cells were incubated in a PBS solution containing 0.1% Triton X-100 and 0.5% acetic acid for 10 min and, after three washings in PBS, in a solution containing 2 μg/mL of the monoclonal anti-α-tubulin antibody (Sigma Chemical Co., St. Louis, MO) for 1 h at RT in a humidified chamber. Following the primary antibody incubation, the cells were washed three times in PBS and incubated with an AlexaFluor-conjugated goat antimouse secondary antibody (Molecular Probes, Leiden, The Netherlands) at a concentration of 20 μg/mL for 1 h at RT in the dark. For nuclear staining, the cells were incubated with Hoechst 33342 (Sigma Chemicals) at a

concentration of 10 μg/mL for 10 min at RT in the dark. Coverslips were then mounted with 50% glycerol in PBS. Cells were analyzed with an epifluorescent microscope (Polyvar, Zeiss AG, Germany) and imaged with a cooled CCD camera (Photometrics, Roper Scientific Inc., CA). Images were then processed with Metamorph software (Universal Imaging, Downingtown, PA).

Acknowledgment. The authors would like to thank Dr. Michel Simard (Université de Montréal) for X-ray analysis and Prof. Stephen Hanessian for critical revision of the manuscript and helpful suggestions.

Supporting Information Available: ^{1}H NMR, ^{19}F NMR, and MS of new derivatives, as well as crystal data for compound **7**. This material is available free of charge via the Internet at http://pubs.acs.org.

References

(1) (a) Pettit, G. R.; Singh, S. B.; Hamel, E.; Lin, C. M.; Alberts, D. S.; Garcia-Kendall, D. Isolation and structure of the strong cell growth and tubulin inhibitor combretastatin A-4. *Experientia* **1989**, *45*, 209–211. (b) Pettit, G. R.; Cragg, G. M.; Herald, D. L.; Schmidt, J. M.; Lobavanijaya, P. Isolation and structure of combretastatin. *Can. J. Chem.* **1982**, *60*, 1347–1376.

(2) Nam, N. H. Combretastatin A-4 analogues as antimitotic anti-tumor agents. *Curr. Med. Chem* **2003**, *10*, 1697–1722, and references cited therein.

(3) (a) Hori, K.; Saito, S. Microvascular mechanisms by which the combretastatin A-4 derivative AC7700 (AVE8062) induces tumour blood flow stasis. *Br. J. Cancer* **2003**, *89*, 1334–1344, and references cited therein. (b) Hori, K.; Saito, S. Induction of tumour blood flow stasis and necrosis: a new function for epinephrine similar to that of combretastatin A-4 derivative AVE8062 (AC7700). *Br. J. Cancer* **2004**, *90*, 549–553. (c) Tozer, G. M.; Prise, V. E.; Wilson, J.; Locke, R. J.; Vojnovic, B.; Stratford, M. R.; Dennis, M. F.; Chaplin, D. J. Combretastatin A-4 phosphate as a tumor vascular-targeting agent: Early effects in tumors and normal tissues. *Cancer Res.* **1999**, *59*, 1626–1634.

(4) Chaplin, D. J.; Hill, S. A. The development of combretastatin A4 phosphate as a vascular targeting agent. *Int. J. Radiat. Oncol., Biol., Phys.* **2002**, *54*, 1491–1496.

(5) Pettit, G. R.; Temple, C, Jr.; Narayanan, V. L.; Varma, R.; Boyd, M. R.; Rener, G. A.; Bansal, N. Antineoplastic agents 322. Synthesis of combretastatin A-4 prodrugs. *Anti-Cancer Drug Des.* **1995**, *10*, 299–309.

(6) Pettit, G. R.; Lippert, J. W. Synthesis of the combretastatin A-1 and combretastatin B-1 prodrugs. *Anti-Cancer Drug Des.* **2000**, *15*, 203–216.

(7) Kirwan, I. G.; Loadman, P. M.; Swaine, D. J.; Anthoney, D. A.; Pettit, G. R.; et al. Comparative preclinical pharmacokinetic and metabolic studies of the combretastatin prodrugs combretastatin A4 phosphate and A1 phosphate. *Clin. Cancer Res.* **2004**, *10*, 1446–1453.

(8) Hatanaka, T.; Fujita, K.; Ohsumi, K.; Nakagawa, R.; Fukuda, Y.; Nihei, Y.; Suga, Y.; Akiyama, Y.; Tsuji, T. Novel B-ring modified combretastatin analogues: syntheses and antineoplastic activity. *Bioorg. Med. Chem. Lett.* **1998**, *8*, 3371–3374.

(9) Ohsumi, K.; Nakagawa, R.; Fukuda, Y.; Hatanaka, T.; Morinaga, Y.; Nihei, Y.; Ohishi, K.; Suga, Y.; Akiyama, Y.; Tsuji, T. Novel combretastatin analogues effective against murine solid tumors: Design and structure−activity relationships. *J. Med. Chem.* **1998**, *41*, 3022–3032.

(10) Lawrence, N. J.; Ghani, F. A.; Hepworth, L. A.; Hadfield, J. A.; McGown, A. T.; Pritchard, R. G. The synthesis of *E*- and *Z*-combretastatin A-4 and a phenantrene from *Combretum caffrum*. *Synthesis* **1999**, *9*, 1656–1660.

(11) Simoni, D.; Grisolia, G.; Giannini, G.; Roberti, M.; Rondanin, R.; Piccagli, L.; Baruchello, R.; Rossi, R.; Romagnoli, R.; Invidiata, F. P.; Grimaudo, S.; Jung, M. K.; Hamel, H.; Gebbia, N.; Crosta, L.; Abbadessa, V.; Di Cristina, A.; Dusonschet, L.; Meli, M.; Tolomeo, M. Heterocyclic and phenyl double-bond-locked combretastatin analogues possessing potent apoptosis-inducing activity in HL60 and in MDR cell lines. *J. Med. Chem.* **2005**, *48*, 723–736.

(12) Wang, L.; Woods, K. W.; Li, Q.; Barr, K. J.; McCroskey, R. W.; Hannic, S. M.; Gherke, L.; Credo, R. B.; Hui, Y. H.; Marsh, K.; Warner, R. L.; Jang, Y.; Zielinski-Mozng, N.; Frost, D.; Rosenberg, S. H.; Sham, H. L. Potent, orally active heterocycle-based Combretastatin A-4 analogues: Synthesis, structure−activity relationship, pharmacokinetics, and in vivo antitumor activity evaluation. *J. Med. Chem.,* **2002**, *45*, 1697–1711.

(13) (a) Cushman, M.; Nagarathnam, D.; Gopal, D.; He, H.-M.; Lin, C. M.; Hamel, E. Synthesis and evaluation of analogues of (*Z*)-1-(4-methoxyphenyl)-2-(3,4,5-trimethoxyphenyl)ethene as potential cytotoxic and antimitotic agents. *J. Med. Chem.* **1992**, *35*, 2293–2306. (b) Tron, G. C.; Pagliai, F.; Del Grosso, E.; Genazzani, A. A.; Sorba, G. Synthesis and cytotoxic evaluation of combretafurazans. *J. Med. Chem.* **2005**, *48*, 3260–3268.

(14) Welch, J. T., Ed. *Selective Fluorination in Organic and Bioorganic Chemistry*; ACS Symposium Series 456: Washington D.C., 1991.

(15) Seebach, D. Organic synthesis-Where now. *Angew. Chem., Int. Ed. Engl.* **1990**, *29*, 1320.

(16) Hertel, L. W.; Ternansky, R. J. *Stud. Org. Chem. (Amsterdam)* **1993**, *48*, 23.

(17) Biffinger, J. C.; Kim, H. W.; DiMagno, S. G. The polar hydrophobicity of fluorinated compounds. *ChemBioChem* **2004**, *5*, 622–627.

(18) Giannini, G. Fluorinated anthracyclines: Synthesis and biological activity. *Med. Chem. Rev.−Online* **2004**, *1*, 47–71.

(19) Ringel, I.; Jaffe, D.; Alerhand, S.; Boye, O.; Muzaffar, A.; Brossi, A. Fluorinated colchicinoids: Antitubulin and cytotoxic properties. *J. Med. Chem.* **1991**, *34*, 3334–3338.

(20) Hadfield, J. A.; McGown, A. T.; Mayalarp, S. P.; Land, E. J.; Hamblett, I.; Gaukroger, K.; Lawrence, J. N.; Hepworth, L. A.; Butler, J. Preparation of substituted stilbenes as antitumor agents, Patent WO02050007, 2005.

(21) Gaukroger, K.; Hadfield, J. A.; Lawrence, N. J.; Nolan, S.; McGown, A. T. Structural requirements for the interaction of combretastatins with tubulin: how important is the trimethoxy unit. *Org. Biomol. Chem.* **2003**, *1*, 3033–3037.

(22) David, P. D. Preparation and use of cis-stilbenes with vascular damaging activity, Patent WO0112579, 2001.

(23) Lawrence, J. N.; Hepworth, L. A.; Rennison, D.; McGown, A. T.; and Hadfield, J. A. Synthesis and anticancer activity of fluorinated analogues of combretastatin A-4. *J. Fluorine Chem.* **2003**, *123*, 101–108.

(24) Ducki, S.; Mackenzie, G.; Lawrence, N. J.; Snyder, J. P. Quantitative structure−activity relationship (5D-QSAR) study of combretastatin-like analogues as inhibitors of tubuline assembly. *J. Med. Chem.* **2005**, *48*, 457–465.

(25) (a) Bellucci, G.; Berti, G.; Chiappe, C.; Lippi, A.; Marioni, F. The metabolism of carbamazepine in humans: Steric course of the enzymatic hydrolysis of the 10,11-epoxide. *J. Med. Chem.* **1987**, *30*, 768–773. (b) Kevin Park, B.; Kitteringham, N. R.; O'Neill, P. M. Metabolism of fluorine-containing drugs. *Annu. Rev. Pharmacol. Toxicol.* **2001**, *41*, 443–470. (c) Aprile, S.; Del Grosso, E.; Tron, G. C.; Grosa, G. In vitro metabolism study of combretastatin A-4 in rat and human liver microsomes. *Drug Metab. Dispos.* **2007**, *35*, 2252–2261.

(26) (a) Giannini, G., Fluorocombretastatin and derivatives thereof, Patent WO05007603, 2005. (b) Drug Data Report, 2005; *27*, 361, and reference therein reported. (c) Tron, G. C.; Pirali, T.; Sorba, G.; Pagliai, F.; Busacca, S.; Genazzani, A. A. *J. Med. Chem.* **2006**, *49*, 3033–3044. (d) Mahindroo, N.; et al. Antitubulin agents for the treatment of cancer - a medicinal chemistry update. *Expert Opin. Ther. Pat.* **2006**, *16*, 647–691.

(27) Simoni, D.; Romagnoli, R.; Baruchello, R.; Rondanin, R.; Rizzi', M.; Pavani, M. G.; Alloatti, D.; Giannini, G.; Marcellini, M.; Riccioni, T.; Castorina, M.; Guglielmi, M. B.; Bucci, F.; Carminati, P.; Pisano, C. Novel combretastatin analogues endowed with antitumor activity. *J. Med. Chem.* **2006**, *49*, 3143–3152.

(28) Ravelli, R. B.; Gigant, B.; Curmi, P. A.; Jourdain, I.; Lachkar, S.; Sobel, A.; Knossow, M. Insight into tubulin regulation from a complex with colchicine and a stathmin-like domain. *Nature* **2004**, *428*, 198–202.

(29) Shimizu, M.; Yamada, N.; Takebe, Y.; Hata, T.; Kuroboshi, M.; Hiyama, T. Generation and carbonyl addition reactions of dibromofluoromethyllithium derived from tribromofluoromethane as applied to the stereoselective synthesis of fluoro olefins and 2-bromo-2-fluoro-1,3-alkanediols. *Bull. Chem. Soc. Jpn.* **1998**, *71*, 2903–2921.

(30) Burton, D. J.; Yang, Z. Y.; Qiu, W. Fluorinated ylides and related compounds. *Chem. Rev.* **1996**, *96*, 1641–1715.

(31) Pettit, G. R.; Moser, B. R.; Boyd, M. R.; Schmidt, J. M.; Pettit, R. K.; Chapuis, J. C. Antineoplastic agents 460. Synthesis of combretastatin A-2 prodrugs. *Anti-Cancer Drug Des.* **2001**, *16*, 185–193.

(32) Pettit, G. R.; Rhodes, M. R.; Herald, D. L.; Hamel, E.; Schmidt, J. M.; Pettit, R. K. Antineoplastic agents. 445. Synthesis and evaluation of structural modifications of (*Z*)- and (*E*)-combretastatin A-4. *J. Med. Chem.* **2005**, *48*, 4087–4099, and references cited therein.

(33) Ismail, F. Important fluorinated drugs in experimental and clinical use. *J. Fluorine Chem.* **2002**, *118*, 27–33.

(34) *Maestro, version 8.0, Impact, version 4.5*, Schrödinger, LLC: New York, NY, 2007.

(35) Goodford, P. A computational procedure for determining energetically favorable binding sites on biologically important macromolecules. *J. Med. Chem.* **1985**, *28*, 849–857.

(36) Jorgensen, W. L.; Tirado-Rives, J. The OPLS force field for proteins. *J. Am. Chem. Soc.* **1988**, *110*, 1657–1666.

(37) Weber, A. E.; Halgren, T. A.; Doyle, J. J.; Lynch, R. J.; Siegl, P. K. S.; Parsons, W. H.; Greenlee, W. J.; Patchett, A. A. Design and synthesis of P2−P1′-linked macrocyclic human renin inhibitors. *J. Med. Chem.* **1991**, *34*, 2692–2701.

(38) Halgren, T. New method for fast and accurate binding-site identification and analysis. *Chem. Biol. Drug Des.* **2007**, *69*, 146–148.

(39) *MacroModel, version 9.5*, Schrödinger, LLC: New York, NY, 2007.

(40) *Spartan'06*, Wavefunction, Inc.: Irvine, CA.

(41) Brinck T. The use of the electrostatic potential for analysis and prediction of intermolecular interactions. In *Theoretical Organic Chemistry, Elsevier Science & Technology*, Eds.; Elsevier: Amsterdam, 1998; vol 5, pp 51–93.

(42) *Glide, version 4.5, Prime, version 1.6*, Schrödinger, LLC: New York, NY, 2007.

(43) Friesner, R. A.; Banks, J. L.; Murphy, R. B.; Halgren, T. A.; Klicic, J. J.; Mainz, D. T.; Repasky, M. P.; Knoll, E. H.; Shelley, M.; Perry, J. K.; Shaw, D. E.; Francis, P.; Shenkin, P. S. Glide: A New approach for rapid, accurate docking and scoring. 1. method and assessment of docking accuracy. *J. Med. Chem.* **2004**, *47*, 1739–1749.

(44) Lyne, P. D.; Lamb, M. L.; Saeh, J. C. Accurate prediction of the relative potencies of members of a series of kinase inhibitors using molecular docking and MM-GBSA Scoring. *J. Med. Chem.* **2006**, *49*, 4805–4808.

(45) Folkman, J.; Haudenschild, C. C.; Zetter, B. R. Long-term culture of capillary endothelial cells. *Proc. Natl. Acad. Sci. U.S.A.* **1979**, *76*, 5217–5221.

(46) Skehan, P.; Storeng, R.; Scudiero, D.; Monks, A.; McMahon, J.; Vistica, D.; Warren, J. T.; Bokesch, H.; Kenney, S.; Boyd, M. R. New colorimetric cytotoxicity assay for anticancer-drug screening. *J. Natl. Cancer Inst.* **1990**, *82*, 1107–1112.

JM701362M